

Extreme Fast Charging of Electric Vehicles: A Technology Overview

Hao Tu^{id}, *Student Member, IEEE*, Hao Feng^{id}, *Member, IEEE*, Srdjan Srdic, *Senior Member, IEEE*,
and Srdjan Lukic^{id}, *Senior Member, IEEE*

Abstract—With the number of electric vehicles (EVs) on the rise, there is a need for an adequate charging infrastructure to serve these vehicles. The emerging extreme fast-charging (XFC) technology has the potential to provide a refueling experience similar to that of gasoline vehicles. In this article, we review the state-of-the-art EV charging infrastructure and focus on the XFC technology, which will be necessary to support the current and future EV refueling needs. We present the design considerations of the XFC stations and review the typical power electronics converter topologies suitable to deliver XFC. We consider the benefits of using the solid-state transformers (SSTs) in the XFC stations to replace the conventional line-frequency transformers and further provide a comprehensive review of the medium-voltage SST designs for the XFC application.

Index Terms—Charging stations, dc fast charger, electric vehicles (EVs), extreme fast charging (XFC), solid-state transformer (SST).

I. INTRODUCTION

AMID growing concerns about climate change, key government and private stakeholders have pushed for moving away from petroleum as the main energy source for powering our transportation system. Transportation systems powered by electricity can help to reduce the consumption of petroleum: battery electric vehicles (EVs) would be plugged into the grid, and their on-board battery systems can be recharged using clean, renewable electricity.

Moving to an electric transportation model requires battery storage capable of supplying the energy and power demands of the vehicle. The Li-ion battery technology has advanced significantly over the last couple of years, making EVs more cost-effective and practical. The cost of the batteries has fallen to less than \$120/kWh [1]–[3]. Despite huge improvements in the energy density of the Li-ion batteries (200–300 Wh/kg) and the significantly higher efficiency of the electric propulsion drivetrain, the driving range of the EVs on one charge is still shorter than the range of the conventional gasoline vehicles due to the orders of magnitude larger (12 000 Wh/kg [2], [4]) energy density of petroleum. In summary, despite the failing

cost and major improvement in performance, Li-ion battery degradation at rest and during cycling, charging rate limitations due to the electrochemical processes, and limited energy density (compared with petroleum) still pose major challenges to more widespread EV adoption [5], [6].

Beyond Li-ion battery technology limitations, a key remaining challenge for the wide adoption of EVs is the lack of the refueling infrastructure that can quickly and seamlessly recharge EV batteries to extend the driving range during longer trips. Therefore, there is an urgent need for an EV charging infrastructure that will parallel the existing gasoline stations, particularly in the regions where long-distance trips are common. However, designing and deploying such an EV charging infrastructure is complex and must consider competing industry standards, available technologies, grid impacts, and other technical and policy issues.

In this article, we first review the state-of-the-art dc fast chargers and present the motivation for and the advantages of grouping dc fast chargers into extreme fast-charging (XFC) stations. We review power electronics converter topologies suitable for XFC stations, specifically focusing on the ac/dc front-end stage design and the isolated and nonisolated dc/dc converter topologies and their applications that satisfy the isolation requirements for automotive traction batteries. Furthermore, we assess the benefits of replacing the conventional line-frequency transformer with the solid-state transformer (SST) in the XFC stations to convert the medium voltage (MV) into low voltage (LV) and provide galvanic isolation. We review the SST topologies for the XFC application proposed in the literature.

II. STATUS OF THE EV CHARGING INFRASTRUCTURE

The Society of Automotive Engineers (SAE) defines the conductive charging methods of the EVs in North America in the SAE J1772 Standard [7]. AC level 1 and ac level 2 on-board chargers take 120- and 240-V ac input, respectively, delivering a peak power of 1.9 and 19.2 kW, respectively. Due to their relatively low-power rating, these on-board chargers are suitable for overnight charging. The limited power ratings of on-board chargers have led to the development of dc fast chargers, typically rated at 50 kW and, more recently, at power levels up to 350 kW. These chargers deliver dc power to the vehicle battery via an isolated power converter located outside the vehicle, and they have the potential to provide EV users with satisfactory charging speed.

Manuscript received September 26, 2019; revised November 14, 2019; accepted November 30, 2019. Date of publication December 10, 2019; date of current version January 7, 2020. This work was supported in part by the U.S. Department of Energy under Award DE-EE0008450. (Corresponding author: Srdjan Lukic.)

The authors are with the Electrical and Computer Engineering Department, North Carolina State University, Raleigh, NC 27606 USA (e-mail: smlukic@ncsu.edu).

Digital Object Identifier 10.1109/TTE.2019.2958709

2332-7782 © 2019 IEEE. Personal use is permitted, but republication/redistribution requires IEEE permission.
See http://www.ieee.org/publications_standards/publications/rights/index.html for more information.

TABLE I
TECHNICAL SPECIFICATIONS OF THE STATE-OF-THE-ART DC FAST CHARGERS

Manufacturer Model	ABB Terra 53	Tritium Veefil-RT	PHIHONG Integrated Type	Tesla Supercharger	EVTEC espresso&charge	ABB Terra HP
Power	50 kW	50 kW	120 kW	135 kW	150 kW	350 kW
Supported protocols	CCS Type 1 CHAdeMO 1.0	CCS Type 1 & 2 CHAdeMO 1.0	GB/T	Supercharger	SAE Combo-1 CHAdeMO 1.0	SAE Combo-1 CHAdeMO 1.2
Input voltage	480 Vac	380-480 Vac 600-900 Vdc	380 Vac \pm 15% 480 Vac \pm 15%	380-480 Vac	400 Vac \pm 10%	400 Vac \pm 10%
Output voltage	200-500 V 50-500 V	200-500 V 50-500 V	200-750 V	50-410 V	170-500 V	150-920 V
Output current	120 A	125 A	240 A	330 A	300 A	375 A
Peak efficiency	94%	>92%	93.5%	91%	93%	95%
Volume	758 L	495 L	591 L	1047 L	1581 L	1894 L
Weight	400 kg	165 kg	240 kg	600 kg	400 kg	1340 kg
Time to add 200 miles	72 min	72 min	30 min	27 min	24 min	10 min

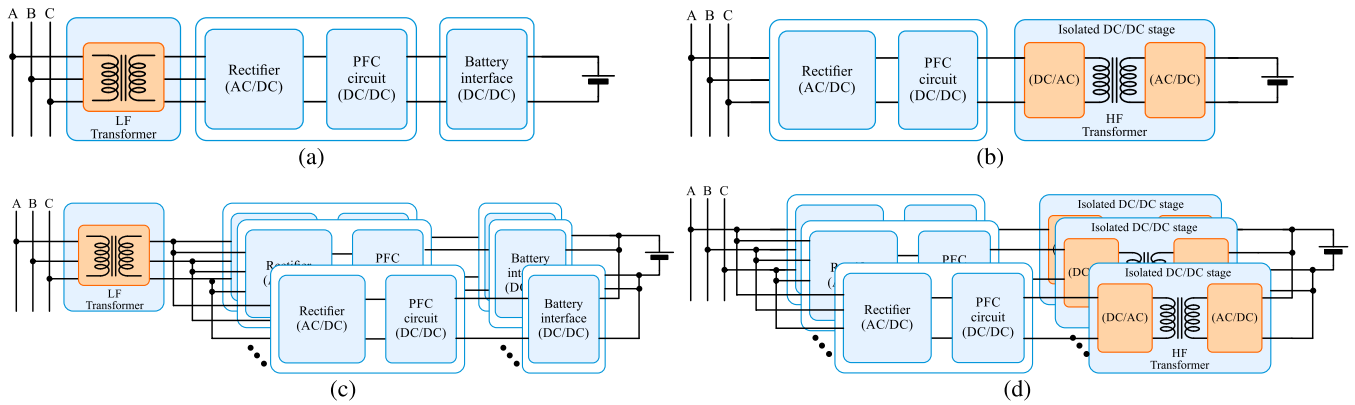


Fig. 1. Simplified block diagram of conventional dc fast charger power conversion systems. (a) Single-module charger with a nonisolated dc/dc converter. (b) Single-module charger with an isolated dc/dc converter. (c) Multiple paralleled modules shown in (a). (d) Multiple paralleled modules shown in (b).

Table I summarizes the state-of-the-art dc fast chargers on the market. The state-of-the-art dc fast chargers convert the three-phase ac voltage up to 480 V into the desired dc voltage by two power electronics-conversion stages: an ac/dc-rectification stage with power factor correction (PFC), which converts three-phase input ac voltage into an intermediate dc voltage, and a dc/dc stage, which converts the intermediate dc voltage into a regulated dc voltage required to charge the EV. The galvanic isolation between the grid and the EV battery can be provided in one of the two following methods. The first option is to use a line-frequency transformer before the ac/dc stage to provide isolation from the grid [see Fig. 1(a)]. The following dc/dc stage is a nonisolated converter. The second option is to exploit a high-frequency transformer inside an isolated dc/dc converter to provide isolation [see Fig. 1(b)]. If a single-module charger does not meet the power requirement of the dc fast charger system, multiple identical modules are connected in parallel to increase the output power, as shown in Fig. 1(c) and (d). An example is the Tesla supercharger, which is made of 12 paralleled modules [8]. A similar approach is used by most manufacturers listed in Table I.

To ensure compatibility, a number of governing bodies have developed standardized protocols and couplers for the dc fast charger system. The five standard dc fast-charging systems

in use are listed in Table II. The IEC 62196-3 Standard [9] defines four different vehicle coupler configurations for dc fast charging: Configuration AA (proposed and implemented by CHAdeMO Association), Configuration BB (also known as GB/T and available only in China), Configuration EE [Type 1 Combined Charging System (CCS), adopted in North America], and Configuration FF (Type 2 CCS, adopted in Europe and Australia). There is also a proprietary system developed by Tesla Inc. and used exclusively for Tesla vehicles.

The power delivered to the EV is limited not only by the charge acceptance of the batteries and the ratings of the charger but also by the connector and the cable between the vehicle and the charger. The connector ratings are defined by the standard, and currently, the CHAdeMO standard supports the highest power capacity. High charging current requires cables with larger diameters to avoid overheating. The cable weight for the 50-kW state-of-the-art fast chargers is about 9 kg [10]. If the battery voltage stays at 400-V level, the cable weight for 200 kW charging can exceed the safety lifting limit for a single person (22.7 kg according to OSHA). One way to reduce the cable weight and deliver more power to the vehicle is to transfer power at higher voltage levels. For 800-V voltage level, the cable weight limits the charging power to be lower than 350 kW [11]. Cable liquid cooling is

TABLE II
DIFFERENT STANDARDS FOR DC FAST-CHARGING SYSTEMS






Standard	CHAdemo IEEE 2030.1.1 IEC 62196-3 (Configuration AA)	GB/T GB/T 20234.3 IEC 62196-3 (Configuration BB)	CCS Type 1 SAE J1772 IEC 62196-3 (Configuration EE)	CCS Type 2 IEC 62196-3 (Configuration FF)	Tesla
Coupler Inlet					
Maximum Voltage	1000 V	1000 V	600 V	1000 V	410 V
Maximum Current	400 A	250 A	200 A	200 A	330 A
Available Power	400 kW	120 kW	150 kW	175 kW	135 kW

TABLE III
EVs ON THE MARKET AND THEIR DRIVING RANGE

Model	Battery Capacity (kWh)	Driving Range (Mile)
Nissan Leaf 62 KWH	62	226
Chevy Bolt EV	60	238
Hyundai Kona Electric	64	258
Tesla Model 3 Long Range	75	310
Tesla Model S 100D	100	370

one potential solution that can effectively reduce the thermal stress on the cable, making smaller and lighter cables feasible for XFC. An alternative might be deploying wireless charging in XFC stations, which eliminates the cable completely. Other advantages of wireless charging include inherent galvanic isolation and convenience. However, wireless charging systems commonly have a lower efficiency and power density than the conductive charging systems [12]–[14]. Wireless charging technology review and discussion are beyond the scope of this article.

III. XFC STATIONS: MOTIVATION, TRENDS, AND CHALLENGES

With the market demand for EVs that can cover most travel scenarios on a single charge, most EVs today are able to provide more than 200-mi driving range. Table III shows the battery capacity and driving range for some of the top selling EVs on the market. Given that the vehicle range is acceptable for many driving scenarios, there is a need for a charging infrastructure that can replenish these batteries in a time commensurate with that of the gasoline refueling experience. Assuming an energy consumption of 30 kWh/100 mi, on-board chargers rated at 7.2 kW would require more than 8 h to add 200-mi range to the EV (assuming the vehicle is charged at constant power). A 50-kW fast charger still needs more than 1 h to add 200 mi, while the 135-kW Tesla supercharger only needs 27 min. The recently proposed 350-kW dc ultrafast chargers can shorten the time of adding 200-mi range to 10 min, which is comparable with the refueling experience of gasoline vehicles.

With the EV charging power increasing, designing, and building, a system that can deliver such high power becomes increasingly challenging and costly. The installation costs of XFC stations can be very high when considering all the

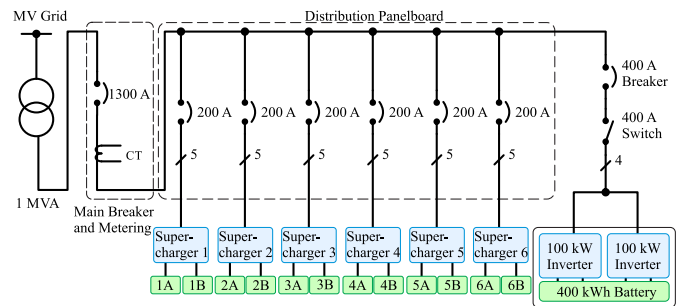


Fig. 2. One line diagram of Tesla supercharger station in Mountain View.

necessary electrical service upgrades such as a transformer and a feeder, condition of the ground surface, conduits from the power source to the service transformer and from the transformer to the fast charger, material costs, permits, and administration. While the installation costs of the dc fast chargers vary from site to site, a significant portion comes from the electrical service upgrades [15]. Consequently, building XFC charging stations with multiple chargers makes more economic sense than building single-port chargers, since some of the site construction overhead is spread over multiple charging ports. With multiple chargers sharing the same upstream equipment, XFC stations' footprint per port can be significantly reduced, allowing for installations in densely populated areas.

With the increasing EV adoption and ever-increasing charging rates, EVs are likely to become a significant new load on the power distribution system and present challenges to the utility. If the EV charging is left uncontrolled, a daily peak load increase and a daily peak load shift due to EV charging may occur, causing transformer and feeder overload, accelerating transformer aging, and increasing power losses [16]–[18]. Furthermore, the chargers' power electronics interface drawing a constant power may have a negative influence on the distribution system stability, cause voltage unbalance, and decrease the power quality [19]. One possible method to mitigate the power demand and reduce the impact of EV charging on the grid is to integrate multiple renewable resources and battery energy-storage systems into XFC stations [20], [21]. An example is the Tesla supercharger station in Mountain View, California, with 200 kW (400 kWh) of battery energy storage, as shown in Fig. 2. Smart charging management coordinating multiple

EVs in a single XFC charging station or multiple XFC stations can help reduce the peak demand of the XFC installation.

Grouping multiple chargers (thus multiple charging EVs) into an XFC charging station makes it possible to schedule vehicle charging and derate the station upstream equipment. As the charging power for an EV is a function of the battery size and its state of charge (SOC), the power demand of the charging station can vary significantly when multiple EVs are charging at the same time. By scheduling the charging of multiple vehicles and exploiting the load diversification resulting from different EV battery capacities and accommodating charge acceptance of the battery as a function of the SOC, the actual system power demand from the grid can be substantially lower than the rated value. If an energy storage system is available at the station, the peak power demand can be further reduced. For example, Bai *et al.* [22] show that the power rating of an XFC station with ten charging slots, each rated at 240 kW, can be set at less than 50% of the rated power, when considering realistic EV arrival times at the station and a realistic distribution of the initial EV battery SOC. If a relatively small storage system is connected to the station, more than 98% of the power demand can be satisfied with an average charging delay time of less than 10 s.

In addition to derating the upstream grid tie equipment and decreasing the installation cost, significant research focuses on exploiting the diversification effect of the vehicle power requirements of multiple EVs charging simultaneously to achieve different objectives such as demand charge reduction, charging cost minimization, charging availability improvement, profit maximization, and so on [23], [24]. In [25], a two-stage coordinated charging strategy for the EV charging stations is proposed. While the first stage tries to maximize the station's profit and provide as much charging availability as possible, the second stage minimizes the peak demand of the station based on the constraints from the first stage. In [26], an online optimization algorithm is proposed for an EV charging station to minimize the charging cost while constraining the power exchange between the grid and the station. The proposed algorithm allows the EV drivers to opt between a fast-charging option to shorten the charging time and a charging option to minimize the cost. Negarestani *et al.* [27] propose an approach to sizing the storage unit for a fast-charging station. The approach can reduce the energy cost and the storage cost while considering the different driving and charging patterns of the EVs. An algorithm proposed in [28] aims at charging multiple EVs to the desired SOC in a given amount of time with the help of vehicle-to-vehicle (V2V) energy transfer. Transferring energy among charging vehicles provides more flexibility in peak demand reduction and cost minimization. However, this requires the chargers in the station to be equipped with bidirectional power flow capability.

In addition to V2V, bidirectional power flow capability enables the vehicle-to-grid (V2G) technology implemented in the EVs to feed power from the vehicles' batteries to the grid. If properly controlled, the on-board batteries of the EVs can be aggregated into an effective energy storage for the XFC station. Furthermore, the XFC station can also be

TABLE IV
COMPARISON OF AC-CONNECTED AND DC-CONNECTED SYSTEMS

	Ac-connected	Dc-connected
Conversion stages	More	Less
Efficiency	Lower	Higher
front-end de-rating	No	Yes
Control	Complex	Simple
Protection	Straightforward	Complex
Metering	Standardized	Non-standardized

a coupling point for renewable energy sources (RES) such as solar and wind [29]. Integrating RES and exploiting V2G technology not only adds generation to the station and mitigates demand charges, but also enables profiling the power exchange between the charging station and the grid and, therefore, provides ancillary services to the grid including load shifting and frequency regulation [30]–[32], reactive power support for voltage regulation [33], [34], and renewable generation firming [35], [36].

Beyond a single station, researchers have looked at utilizing vehicle-to-infrastructure (V2I) communication, to route the EVs to the stations that have available capacity, or where their load would present the least stress on the power grid. For example, [37] proposes a publish/subscribe communication framework for EVs, roadside units, and charging stations. The roadside units pass messages between the EVs and the stations and assist the EVs in locating and reserving the least congested stations. In [38], instead of roadside units, public transportation buses are used as brokers between the message publisher (charging station) and the subscriber (EVs) to assist EVs in finding the fastest route to destination. In [39], a power allocation scheme for EV charging stations is proposed. By allocating power to different charging stations and routing EVs, the stations' profitability is increased while providing better quality of service to the EV drivers. Another important aspect is the optimal placement of EV charging stations. For example, in [40], the optimal locations and capacities of EV charging stations are determined through a spatial-temporal model of the EV mobility, reducing the planning cost and improving the charger availability.

IV. XFC STATION CONCEPTS AND CONVERTER TOPOLOGIES

The local distribution network among multiple chargers, local RES, and energy storage can be ac or dc, as shown in Fig. 3(a) and (b), respectively. Each approach has a number of advantages and challenges, as summarized in Table IV. The sections below outline these challenges and opportunities, and review the implementation approaches for both types of charging stations. Different power electronics converters for XFC application are identified and compared. Their advantages and disadvantages are discussed. Topology variations and control improvements proposed in literature to better suit XFC are also discussed. Note that this article focuses on the converter topologies suitable for XFC application and does not cover the topologies for on-board chargers. Reviews of on-board

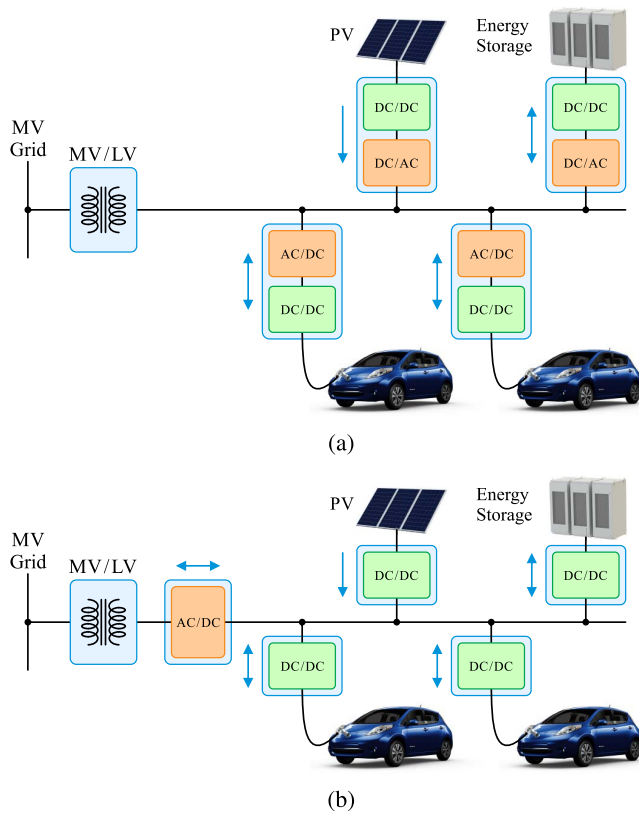


Fig. 3. Configurations for XFC stations. (a) AC-connected system. (b) DC-connected system.

chargers, integrated chargers, and off-board chargers can be found in [41] and [42].

A. XFC Stations With AC and DC Power Distribution

For the ac-connected systems, a step down-transformer interfaces between the distribution network and a three-phase ac bus operating at 250–480-V line-to-line voltage. The ac bus supplies each charger at the station, and each charger features a separate ac/dc stage. This approach significantly increases the number of conversion stages between the distribution network and the dc port of the EV or the RES (e.g., PV or battery). Having more conversion stages in the ac-connected system increases the system complexity and cost while decreasing the system efficiency. The advantages of using the ac bus include the availability and maturity of the rectifier and inverter technology, availability of the ac switchgear and protective devices, and well-established standards and practices for the ac power distribution systems. Furthermore, there are developed standards for EV charging stations such as [43]–[45]. Most state-of-the-art XFC stations are ac-connected systems, for example, the Tesla supercharger station in Mountain View, California, shown in Fig. 2, and the ABB dc fast-charging station in Euroa, Victoria, Australia [46].

For the dc-connected systems, one central front-end ac/dc converter is used to create a dc bus, providing a more energy efficient way of interfacing dc energy storage and RES. The central front-end features a low-frequency transformer followed by an LV (250–480 V) rectifier stage or an SST that provides the rectification, voltage step-down, and isolation

function in a single unit. To accommodate the state-of-the-art battery voltage range (approximately 400 V), the dc bus voltage is normally less than 1000 V. At this voltage level, the design of the XFC stations with a dc bus should comply with the same standards as XFC stations with an ac bus [43]–[45]. Each charger is interfaced between the dc bus and a dc/dc converter, removing the individual ac/dc converters. With a reduced number of conversion stages, the system efficiency is improved compared with that of the ac-connected systems. One potential advantage of the “dc distribution” approach is that there is a single interconnection to the utility though the central front end. This provides an opportunity to exploit the load diversification resulting from varying EV battery capacities and changing charge acceptance of the battery as a function of the SOC to significantly derate the ac/dc converter and the nameplate of the grid connection, thus reducing the system installation cost. Other advantages of the dc systems include the absence of reactive power in dc systems, which simplifies control [47]. The single inverter interconnection with the grid also simplifies islanding from and connection to the main grid. Another potential advantage of the dc distribution systems is the opportunity to use partial power converters to interface between the dc bus and the vehicle [48]–[51]. These partial power converters only process a portion of the power delivered to the vehicle, reducing the converter ratings and thus cost and improving the conversion efficiency. For example, in [50] and [51], different partial power dc/dc converters are proposed to interface to a common dc bus of an XFC station. Since a portion of the power in these converters passes directly from the dc bus to the vehicle, these converters cannot provide galvanic isolation between the vehicles. Thus, this approach has significant technical hurdles to overcome to meet the relevant charging standards in existence today, which requires that “each output circuit shall be isolated from each other for an EV charging station [44].

Despite its advantages, a dc-connected system presents unique challenges such as dc protection and dc metering. While there are available protective devices for LV dc systems including fuses, circuit breakers, solid-state circuit breakers, and protective relays [52], there are no established standards for protection coordination in the dc-connected EV charging stations. The protection coordination for the dc-connected systems is a complex function of the grounding configuration, fault type, system topology, component specification, size, and so on/ [53]. This issue becomes even more complicated if the chargers are bidirectional. Because a dc-connected system has limited inertia, it is sensitive to disturbance and might become unstable without fast fault clearance. As a result, the speed of fault detection and isolation is critical to system restoration. Studies on existing dc power distribution systems, such as LV dc microgrids, provide guidelines for the protection coordination of dc-connected charging stations. In [54], a protection strategy is presented for an LV dc microgrid considering the coordination between different protective devices. In [55], a protection scheme is proposed for dc systems with a loop-type bus. The proposed scheme is able to detect and isolate the fault and provide power uninterruptedly.

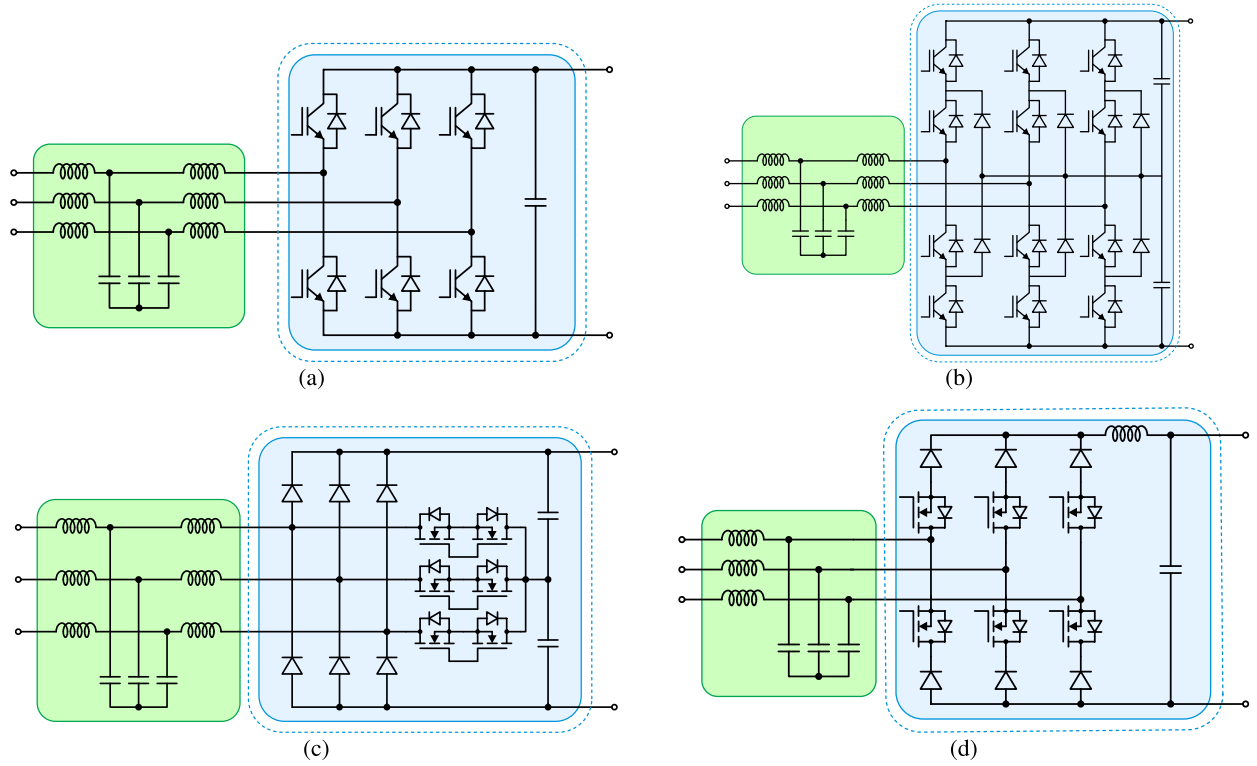


Fig. 4. AC-DC front-end topologies for dc fast chargers. (a) Three-phase PWM rectifier. (b) NPC rectifier. (c) Vienna rectifier. (d) Buck-type rectifier.

TABLE V
COMPARISON OF DIFFERENT AC/DC CONVERTER TOPOLOGIES FOR DC FAST CHARGERS

Converter	Switches/Diodes	Bidirectional	THD	PF Range	Control Complexity
PWM Converter (Fig. 4a)	6 / 0	Yes	Low	Wide	Low
NPC Converter (Fig. 4b)	12 / 6	Yes	Very Low	Wide	Moderate
Vienna Converter (Fig. 4c)	6 / 6	No	Very Low	Limited	Moderate
Buck-type Converter (Fig. 4d)	6 / 6	No	Low	Limited	Low

In the dc-connected system, dc meters need to be installed to measure the energy generation and consumption of the RES, battery energy storage, and EV chargers. This information is critical to the accurate billing of the EV station users and may be used for future station planning [56]. While dc meters are commercially available, there is no established accuracy, calibration, and testing procedures that would allow these units to be used for metering. Developing such a standard and certified dc meters is necessary for the dc-connected systems.

B. Grid-Facing AC/DC Converters

Grid-facing ac/dc converters provide an interface between the grid and a regulated dc bus. A key performance requirement for these converters is high power quality on the ac and dc sides, achieved by input current shaping and output-voltage regulation [57], [58]. In this article, the ac/dc converters suitable for XFC are identified and shown in Fig. 4. Their features are summarized in Table V. They are further categorized as bidirectional and unidirectional converters.

1) *Bidirectional AC/DC Converters*: The most widely used grid-facing ac/dc converter is the three-phase active

pulsewidth-modulated (PWM) converter with an *LCL* filter shown in Fig. 4(a). This boost-type converter has an output voltage higher than the input line-to-line peak voltage. The six-switch PWM converter generates low-harmonic input currents, provides bidirectional power flow, and enables arbitrary power factor (PF) regulation. Due to the simple structure, well-established control schemes, and the availability of low-cost IGBT devices with sufficient current and voltage ratings, this topology is widely adopted in the state-of-the-art dc fast chargers [59].

Another boost-type converter implementation is the neutral-point-clamped (NPC) converter shown in Fig. 4(b). This three-level converter enables the utilization of devices with lower voltage rating that can provide lower switching losses at an acceptable cost. Moreover, the resulting three-level voltage waveform reduces the input current harmonics and dv/dt . In [60], a 30-kW EV charger prototype with an NPC front end achieves low total-harmonic distortion (THD) input current with the leakage inductance of input transformer serving as the ac-side filter. Another advantage of using an NPC converter as the ac/dc front end is that it explicitly creates a bipolar dc bus [61]. This property is explored in [62] and [63] to

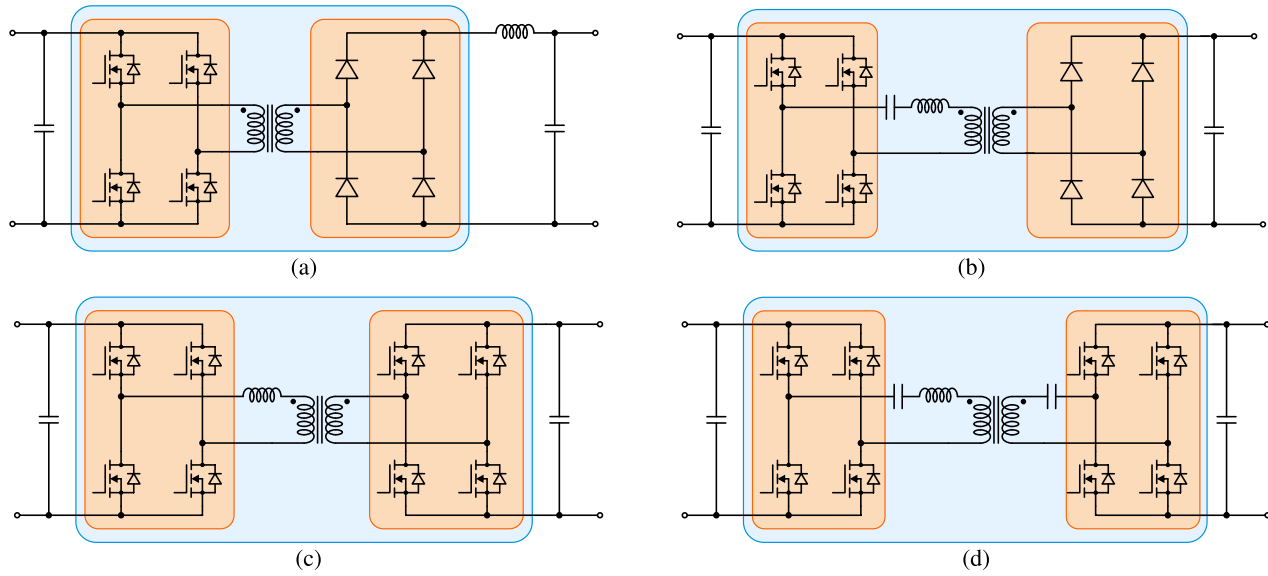


Fig. 5. Isolated dc-dc converter topologies for dc fast chargers. (a) PSFB converter. (b) *LLC* converter. (c) DAB converter. (d) *CLLC* converter.

implement an EV charging station with a bipolar dc bus, allowing the dc/dc converters to connect to half of the dc bus voltage. The availability of a bipolar dc bus also provides opportunities for the partial-power converter implementation for the dc/dc stage; this approach is reviewed in detail in Section IV-A.

2) *Unidirectional AC/DC Converters*: If only unidirectional power flow is required, the T-type Vienna rectifier, shown in Fig. 4(c), is a three-level solution with a reduced number of active switches. While it preserves all the advantages of three-level converters, it also shares the common issues of three-level converters including the need for dc-link capacitor voltage balancing. One major limitation for the Vienna rectifier is the unidirectional power flow and the limited reactive power control. Due to the restricted modulation vector, the range of the achievable reactive power is narrow and depends on the output voltage (the range is $-30^\circ < \phi < 30^\circ$ when the output voltage is higher than twice the peak input ac line-to-line voltage, and it is reduced to $\phi = 0$ if the output voltage is equal to the peak input ac line-to-line voltage). Reference [64] presents a 25-kW EV charger prototype with a single-switch Vienna rectifier and four parallel three-level dc/dc. In [65], a 20-kW SiC-based Vienna rectifier switching at 140 kHz is 98.6% efficient and features compact passive components. In [66], an EV charger is proposed that uses a Vienna rectifier and two isolated dc/dc converters with each dc/dc converter interfaced to half of the dc bus voltage. By using the dc/dc converters to inject the sixth-order harmonic in the dc bus voltage, only one phase of the Vienna rectifier is PWM at a time, improving the system efficiency.

If the output voltage is lower than the input line-to-line voltage, a buck-type unidirectional ac/dc converter shown in Fig. 4(d) can be used. This converter has some advantages over the boost-type topologies, such as inherent short-circuit protection, simple inrush current control, and lower output voltage. An additional advantage is that the input current can

be controlled in an open loop. The power flow can be reversed only if the output voltage is reversed. Thus, the converter is only unidirectional with a fixed output-voltage polarity. The achievable phase difference between the input voltage and the input current fundamental depends on the required output voltage. In order to achieve a higher phase difference, the converter needs to operate with a reduced output-voltage range (i.e., if the wide output-voltage range is required, the phase shift between the input voltage and the input current fundamental needs to be kept small). The conduction losses are generally higher for the boost-type converter, because more devices are connected in series [67], but the switching losses can be lower. The buck-type converter can still operate at very high efficiency, as reported in [68], where 98.8% efficiency was achieved. In [69], the buck-type rectifier is modified to allow two input phases connecting to each phase leg. With two phase legs conducting the current [in contrast to one phase leg for the buck-type rectifier shown in Fig. 4(d)], the device conduction loss is reduced while maintaining low THD of the input current. Adding a fourth diode bridge leg connected to the midpoint of the diode bridge and the star-point of the input capacitors leads to reduced voltage stress on the switches [70]. This allows the use of switches with lower voltage rating and better performance, potentially achieving higher system efficiency.

C. Isolated DC/DC Converters

A dc/dc converter after the ac/dc front end provides an interface to the RES, battery energy storage, or EV battery. Since the EV's battery must not be grounded (i.e., it must be floating with respect to the ground) at all times, galvanic isolation is required to maintain the isolation between the grid and the battery so that the battery protection remains unaffected by the charging system. This can be achieved by using an isolated dc/dc converter. Isolated dc/dc converter topologies suitable for EV chargers are presented in Fig. 5; their features

TABLE VI
COMPARISON OF DIFFERENT ISOLATED DC/DC CONVERTER TOPOLOGIES FOR DC FAST CHARGERS

Converter	Switches/Diodes	Bidirectional	Major Advantages and Disadvantages
PSFB converter (Fig. 5a)	4 / 4	No	Simple Control; wide output range. High switching losses in primary switches and output diodes; duty-cycle loss; hard to realize ZVS under light-load.
LLC converter (Fig. 5b)	4 / 4	No	Low reactive current; ZVS on primary side and ZCS on secondary side. Limited controllability; hard to maintain high efficiency and ZVS under wide operating range
DAB converter (Fig. 5c)	8 / 0	Yes	Wide achievable output range. Inherent reactive current; trade-off between reactive power and ZVS condition
CLLC converter (Fig. 5d)	8 / 0	Yes	Low reactive current; wide ZVS range. Limited controllability under wide output range

are summarized in Table VI. A more comprehensive review of the isolated dc/dc converters is provided in [71] and [72].

1) *Unidirectional Isolated DC/DC Converters*: If only unidirectional power flow is required, a possible implementation is the phase-shift full-bridge (PSFB) converter, shown in Fig. 5(a). When the converter operates in phase-shift PWM control, its active switches operate at zero-voltage switching (ZVS) turn-on [73]. The main disadvantages of this topology are the turn-off losses in the active switches, high losses in the output diodes, and large ringing across the output diodes due to the *LCL* resonance of the transformer leakage inductance and the parasitic capacitance of the reverse-biased diodes and the output inductor. To reduce the voltage overshoot and the ringing, active [73] or passive [74] snubber circuits can be applied at the cost of reduced system efficiency. In [75] and [76], a current-fed PSFB converter is proposed by moving the output inductor to the primary side of the transformer and connecting the diode bridge to an output capacitor directly. This approach minimizes the voltage overshoot and the ringing, but the ZVS range becomes highly load-dependent. To maintain ZVS over a wide operating range for EV battery charging, trailing-edge PWM is used in [75], while auxiliary circuits are proposed in [76]. Similar auxiliary circuits are used in [77] to achieve ZVS for the PSFB converter from the no-load to full-load condition of an EV charger.

Another unidirectional isolated dc/dc converter for XFC is the *LLC* resonant converter, shown in Fig. 5(b). The converter output voltage is regulated by changing the switching frequency to adjust the impedance ratio of the resonant tank to equivalent load. The *LLC* converter uses the magnetizing current to achieve ZVS, resulting in low turn-off losses and low transformer losses [78]. The *LLC* converter can achieve very high efficiency if the input-to-output voltage ratio is narrow [79]. However, it suffers from limited light-load power regulation capability and the ZVS condition may not hold for a wide operating range, thus negatively affecting the efficiency.

Multiple approaches are proposed to improve the performance for a wide output-voltage range and at light load conditions. Various control methods are proposed including PWM, phase shift, and other hybrid modulation schemes to narrow the range of operating frequency while broadening the

output range [80], [81]. In [82], a variable dc voltage is regulated by the ac/dc converter to match the EV battery voltage, allowing the *LLC* converter to always operate around the resonant frequency with maximum efficiency. Although this method is simple and effective with no extra hardware, a wide output-voltage range is not guaranteed, since the dc voltage variation is limited by the grid-voltage and switch-voltage rating. Hardware modifications include employing multiple transformers [83] and multiple rectifiers on the transformer secondary side [84]. In [85], an extra capacitor paralleled with a four-quadrant switch is inserted in the *LLC* resonant tank. By modulating the four-quadrant switch, the inserted capacitance and, therefore, the resonant frequency adapt to the load, improving the efficiency at light-load condition. Despite their effectiveness, these methods require additional hardware and result in higher system cost and larger system volume. In addition, a smooth transition between multiple configurations during operation is difficult to achieve.

Another issue for the *LLC* converter is that the resonant capacitor has to withstand high-voltage stress at high power, which complicates component selection. To enhance the power rating and alleviate the stress on switching devices and resonant components, a multilevel *LLC* converter [86], a three-phase *LLC* converter [87], and an *LLC* converter with paralleled modules [88] can be used.

2) *Bidirectional Isolated DC/DC Converters*: If bidirectional power flow is required, a dual active bridge (DAB) converter [shown in Fig. 5(c)] can be used for EV charging applications due to its high power density, high efficiency, buck and boost capability, low device stress, small filter components, and low sensitivity to component variation [89]–[96]. When introduced in 1991 [96], the DAB converter was not widely adopted due to the high power losses and relatively low switching frequency of the power semiconductor devices at that time. More recently, the DAB converter started gaining attention, due to the capabilities of the new SiC- and GaN-based power semiconductor devices and the advances in the nanocrystalline and amorphous soft magnetic materials, which enabled the converter efficiency and power density improvements [97]. In the DAB converter, the power flow is controlled by adjusting the phase shift between the

primary and the secondary voltage, with transformer leakage inductance serving as the power-transfer element. Owing to its simple structure and ZVS operation, the DAB converter has been extensively used in isolated bidirectional dc/dc conversion applications [98], [99].

For EV battery charging, the converter is required to operate with a wide range of voltage gain and power due to the EV charging profile, under which reactive power can increase dramatically and ZVS condition no longer holds [100]. This causes a dilemma in the design of leakage inductance, in which high leakage benefits a wide ZVS range but worsens the reactive power and results in lower efficiency, and vice versa [101]. To improve the performance under a wide operating range, various modulation schemes have been proposed. Zhao *et al.* [102] propose dual-phase-shift (DPS) modulation to minimize the current stress of the switching devices, where the primary and secondary duty cycles are introduced as an additional degrees of freedom. In [103], the DPS is adopted to achieve ZVS under full load range. In [104] and [105], the concept of DPS is further extended to triple-phase shift (TPS) to enable more degrees of freedom and achieve multiple design objectives such as broader ZVS range, lower current stress, and improved efficiency. In addition, hybrid modulation incorporates operating frequency and pulse density to regulate the transferred power without sacrificing ZVS while controlling the reactive power flow [106], [107]. Recent work in [108] applies TPS to enhance light-load efficiency while switching to DPS to reduce the circulating current under the medium- and heavy-load conditions. However, all proposed control strategies have inherent performance tradeoffs and require complex modulation schemes that may be difficult to implement and may not be as robust to parameter variation. Another concern is the high-frequency charging ripple resulting from the reactive power that is inherent to the DAB converter operation [94].

Another variant of the bidirectional dc/dc converter is the *CLLC* converter shown in Fig. 5(d) [109], [110]. Due to its symmetrical circuit, the *CLLC* converter provides the same voltage gain characteristic in both power flow directions, which reduces the control complexity and facilitates power regulation. Moreover, the *CLLC* converter distributes two resonant capacitors on both sides of the transformer, which helps reduce the resonant capacitor voltage stress compared with the *LLC* converter [111]. Compared with the DAB converter, the leakage inductance required for the *CLLC* resonant tank is much smaller. As a result, the reactive power circulating in the converter is also smaller. Furthermore, the sinusoidal resonant current of the *CLLC* converter exerts smaller stress on the high-frequency transformer than the DAB converter [112]. However, due to its similarities in the *LLC* converter, the *CLLC* converter exhibits similar design tradeoffs as the *LLC* converter such as the ZVS condition and efficiency degradation for a wide voltage and power operating range. The controllability of the *CLLC* converter is another challenge, as the voltage gain curve against frequency tends to be steady in specific frequency ranges [109]. To solve the above issues, Wang *et al.* [113] add an auxiliary transformer to help realize full-load-range ZVS while improving power

regulation. A detailed parameter design methodology is provided in [114] to realize robust power regulation with a wide operating range. Li *et al.* [115] present a design procedure that handles wide voltage gain requirements, and integrated magnetic components are used to improve the power density.

In many cases, there is a desire to minimize the number of active devices in a topology. One way to achieve this is to use the half-bridge equivalents of the converters shown in Fig. 5 including the widely used half-bridge *LLC* converter [116], [117] and the dual half-bridge (DHB) converter [118]–[120]. The half-bridge converters use only four active switches, which reduces the cost. Comparing with the full-bridge version, the voltage applied is half of the dc link voltage. This feature is beneficial to the high-frequency transformer design when used in MV applications. However, the current stress on the active devices is doubled, and the degrees of freedom available for converter control are reduced.

D. Nonisolated DC/DC Converters

If the charging system is designed to exploit the isolation provided by a different power conversion stage of the XFC system (for example, the line-frequency transformer before the ac/dc front end), a nonisolated dc/dc converter can be used instead of an isolated one, while still providing a floating power supply to the vehicle battery. In this discussion, we consider bidirectional nonisolated dc/dc converters for two reasons. First, the achievable efficiency of bidirectional converters is higher than the unidirectional ones due to synchronous rectification. Second, unlike the isolated dc/dc converters, the bidirectional operation does not add more complexity to the control of the nonisolated dc/dc converters. Although focusing on the bidirectional converters, the discussions also apply to the corresponding unidirectional versions.

Considering that the battery voltage is lower than the output voltage of the ac/dc front end in most cases, a boost converter (from the battery point of view) in Fig. 6(a) is the simplest nonisolated topology to interface with the battery. The power rating of this converter is limited, since the current is carried by a single switch. In addition, the inductor size is large if the current ripple needs to be small.

To increase the current-carrying capability and reduce the current ripple seen by the battery, two or more phase legs can be interleaved to form a multi-phase interleaved boost converter. Fig. 6(b) shows an interleaved boost converter with three phase legs. Due to its simple structure, good performance, and scalability to high power, this topology has been widely explored in literature for EV charging application [59], [60], [121]–[123]. In [60], an EV charger prototype is reported to have six phase legs connected in parallel and interleaved to reach 30 kW. In [122], a 100-kW three-phase interleaved boost converter is designed to work in the discontinuous conduction mode (DCM). The inductors are small enough to allow both positive and negative currents in one switching period, achieving ZVS for all switches. With an optimized inductor design, the system size can be reduced and efficiency improved. In [123], an interleaved boost converter implementation operating in DCM uses the partial power concept by

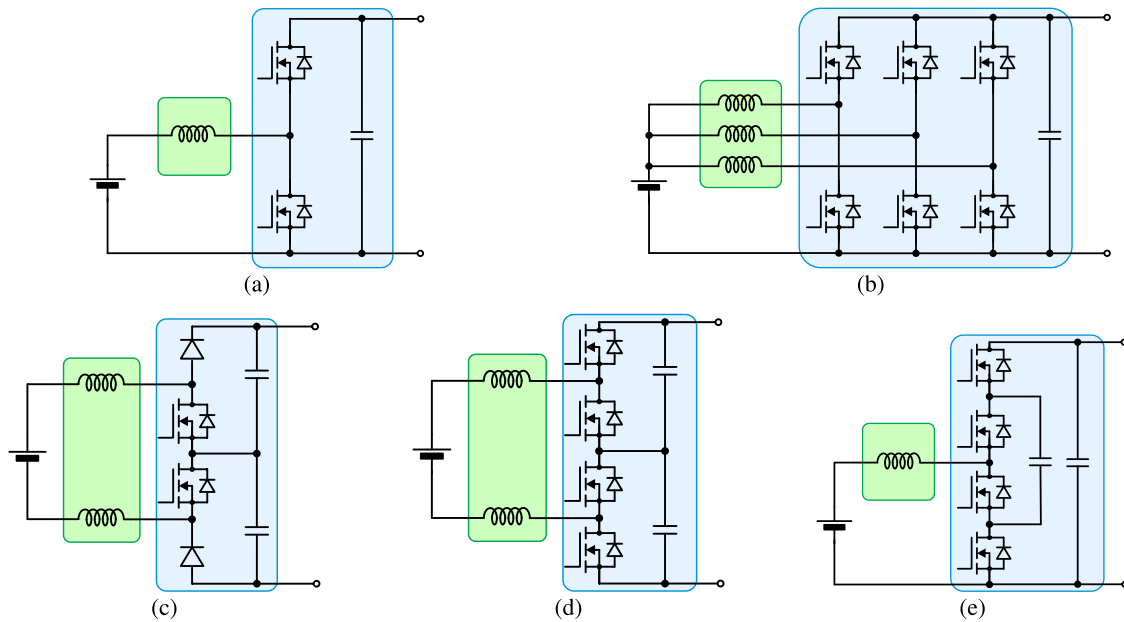


Fig. 6. Nonisolated dc-dc converter topologies for dc fast chargers. (a) Boost converter. (b) Interleaved boost converter. (c) Unidirectional three-level boost converter. (d) Bidirectional three-level boost converter. (e) Three-level flying capacitor converter.

separating the bus voltage into two parts in series. With the converter connecting to part of the bus voltage, switches with lower voltage ratings can be used, potentially reducing the losses. The drawback of this method is the extra hardware and control effort to balance the two dc bus voltages.

Another topology that offers better harmonic performance than the boost converter is the three-level boost converter [124] and its bidirectional version [125], as shown in Fig. 6(c) and (d), respectively. The current ripple in the three-level boost converter is only one-fourth of that in the boost converter if the same inductor is used, which implies a smaller inductor can be used to meet the current ripple specifications. In [126], the performance of a boost converter, a two-phase interleaved boost converter, and a three-level boost converter is compared. This article shows that the three-level boost converter can increase the efficiency and reduce the size of the magnetic components. However, the three-level boost converter has high electromagnetic interference (EMI) in terms of common-mode noise, which could have a negative impact on the battery system. Furthermore, the three-level boost converters cannot be paralleled easily. If there is a phase shift between paralleled three-level boost phase legs, large circulating currents will result unless interphase inductors are used between the phase legs. For high-power applications when multiple parallel phase legs are necessary, circulating currents can be suppressed by either switching the phase legs synchronously [127], which eliminates the inductor size reduction due to interleaving, or using an integrated inductor that suppresses the circulating currents [128]. Due to its three-level nature, the three-level boost converter is suitable for interfacing the EV battery with a bipolar bus such as the EV charging station topologies proposed in [22], [129], and [130].

Another potential three-level topology for fast chargers is a flying capacitor converter shown in Fig. 6(e). This three-level

topology allows for the use of a smaller inductor than a boost converter. In addition, the power rating of the converter can be easily increased by paralleling and interleaving multiple phase legs. However, the short-circuit protection design is challenging due to the presence of the flying capacitor. In addition, the switching commutation loop of the flying capacitor converter involving the uppermost and lowermost devices is larger than that of the boost converter and the three-level boost converter [131], which may cause undesired voltage overshoot during switching. In [132], a 55-kW flying capacitor converter prototype boosts the battery voltage three times to the traction inverter bus voltage. The efficiency is above 96.5% over the entire power range. However, to the best of our knowledge, currently, no proposed or implemented dc fast charger uses the flying capacitor converter.

V. SST-BASED MV EXTREME FAST CHARGERS

The state-of-the-art fast-charging stations are supplied from the three-phase LV distribution grid, using up to 480-V line to line (depending on the region) as an input. This voltage is typically generated by a dedicated MV-to-LV service transformer. The bulky service transformer increases the size and cost of the system while adding complexity to the installation. To eliminate the need of the MV-to-LV transformer, a power electronics-based SST can be used to interface the MV grid directly. The term SST has been loosely used to refer to the concept of replacing line-frequency transformers with power electronics converters that provide voltage conversion and galvanic isolation using high-frequency transformers. Compared with the traditional line-frequency transformer, the SST has a number of unique features such as better controllability, current limiting capabilities, and higher efficiency at light load [133]. Many SSTs proposed in literature convert the MV

TABLE VII
COMPARISON OF DIFFERENT NONISOLATED DC/DC CONVERTER TOPOLOGIES FOR DC FAST CHARGERS

Converter	Switches/Diodes	Major Advantages and Disadvantages
Boost converter (Fig. 6a)	2 / 0	Simple control. Limited current and voltage capability.
Interleaved boost converter (Fig. 6b)	6 / 0	Increased current capability; low current ripple; simple control; good scalability. Limited voltage capability.
Three-level boost converter (Fig. 6d)	4 / 0	Increased voltage capability; reduced current ripple. Not for interleaving due to circulating current.
Flying capacitor converter (Fig. 6e)	4 / 0	Increased voltage capability; good scalability. Difficult short-circuit protection.



Fig. 7. Comparison of the state-of-the-art dc fast charger station to the SST-based solution. Both stations are rated at 675 kW.

ac input into an LV ac output by three conversion stages. The first stage is an active front end that rectifies the line-frequency MV ac input into dc voltage. Then, an isolated dc/dc stage converts the dc voltage to create a dc bus at a desired voltage level while providing galvanic isolation. The final stage inverts the dc voltage into a line-frequency LV ac output. Although other designs such as the single-stage SST proposed in [134] are possible, the three-stage design explicitly creates a dc bus that can interface PVs, battery energy storage systems, EVs, and other dc sources and loads [135], [136]. SST topologies and implementations are summarized and compared in [137] and [138].

In the context of XFC, the SST converts the MV ac voltage into an LV dc voltage while providing galvanic isolation by using a high-frequency transformer inside the SST. As the operating frequency of the high-frequency transformer is much higher than the service transformer (tens of kilohertz versus line frequency), the size of the high-frequency transformer is much smaller than that of the service transformer. Replacing the traditional low-frequency transformer and rectifier with an SST provides higher conversion efficiency and significant space savings compared with the state-of-the-art approach. The higher efficiency leads to power savings for the infrastructure owner that can be passed on to the EV owner. The reduced system footprint provides better utilization of the charging station site. This becomes increasingly important as the charging capabilities of the EV batteries improve, and the penetration of EVs increases. A comparison of the state-of-the-art dc fast charger station (based on a Tesla Supercharger station design) with the SST-based solution in Fig. 7 shows that the SST-based station has a much smaller footprint for the same power rating.

A. SST Designs for EV Charging Applications

Although many SST implementations have been proposed in the literature, this article focuses on the systems that are specifically designed for the XFC application, in which they provide rectification, voltage step-down, and isolation function. Most SST-based MV dc fast chargers proposed in literature are implemented as single-phase single-port units that connect directly to EVs. However, they can also serve as the central ac/dc front end in a dc-connected XFC station with adequate modifications. Furthermore, three-phase implementations can be realized by connecting three identical single-phase converters in a delta or wye form.

SSTs commonly use identical modules as building blocks to reach the desired voltage and power levels. To interface with the MV grid directly, the modules are connected in series at the input to increase the voltage blocking capability, while the outputs of the modules are connected in parallel to provide large output current at the desired low dc voltage. Fig. 8(a) shows the MV fast charger topology developed by the Electric Power Research Institute (EPRI) and Virginia Tech [139], [140]. Three modules are connected in series at the MV ac side (2.4 kV) and in parallel at the battery side. Each module has a unidirectional NPC ac/dc front end to realize ac/dc conversion and PFC. The internal bus of each module operates at 1250 V, allowing off-the-shelf silicon IGBTs or SiC MOSFETs to be used. Following the unidirectional NPC ac/dc front end, two input-series-output-parallel PSFBs convert the internal dc bus voltage into the desired output voltage. One demerit of this topology is that it uses a large number of active switches, which increases the system cost and limits the achievable efficiency and compactness. Furthermore, the output of the

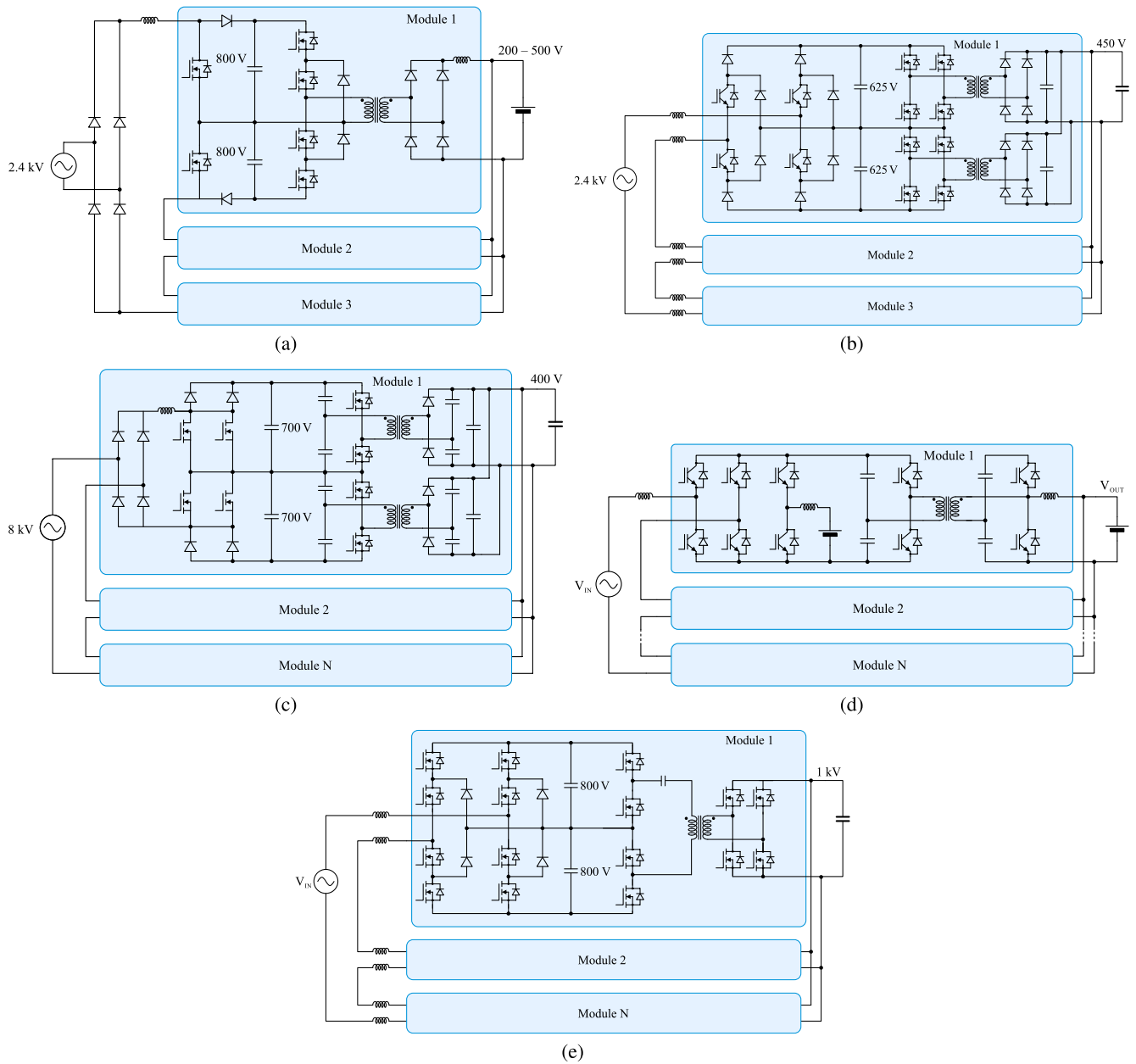


Fig. 8. MV dc fast chargers based on modular SSTs. (a) MV dc fast charger proposed in [139]. (b) MV dc fast charger proposed in [141]. (c) MV dc fast charger proposed in [142]. (d) MV dc fast charger proposed in [143]. (e) MV dc fast charger proposed in [144].

PSFBs is fixed at 450 V. If the converter is connected to an EV, an additional dc/dc stage is necessary to follow the battery charging profile. In the design, a six-phase interleaved boost converter (from the battery point of view) is used to integrate the EV battery. The system efficiency is close to 96% at 38 kW.

Fig. 8(b) shows the topology proposed in [141]. Eight modules are connected in series at the MV side to share the 8-kV ac voltage. The ac/dc front end of each module has an uncontrolled diode bridge rectifier followed by two unidirectional three-level boost converter phase legs in parallel. The internal bus is 1.4 kV. The dc/dc stage is two input-series-output-parallel half-bridge LLC converters capable of soft-switching. To achieve high efficiency, the LLC converters operate in open loop with 100% duty cycle, while the output

voltage is regulated by the ac/dc front end adjusting the bus voltage. This control strategy leads to a narrow output-voltage range that may not be able to meet the EV charging profile. If connected directly to an EV, a subsequent dc/dc converter is necessary to accommodate the battery voltage. The system efficiency is about 97.5% at a rated load of 25 kW.

At North Carolina State University, a 50-kW MV fast charger is developed based on the topology shown in Fig. 8(c) [142], [145]–[147]. Three modules are connected in series at the MV side to share 2.4-kV ac voltage. Instead of having a diode bridge for each module as in the design in Fig. 8(b), a single diode bridge is used to rectify the MV ac input. This reduces the forward voltage drop on diodes and improves the efficiency. Each module has a three-level boost converter for

TABLE VIII
COMPARISON OF DIFFERENT MV DC FAST CHARGERS

Topology	Switches/Diodes/Transformers in One Module	Major Advantages and Disadvantages
[139] (Fig. 8a)	12 / 16 / 2	Modular design. Poor switch utilization; unidirectional. fixed output.
[141] (Fig. 8b)	8 / 12 / 2	Modular design; good switch utilization; high efficiency. Narrow output range; unidirectional operation; fixed output.
[142] (Fig. 8c)	6 / $8 + \frac{4}{3}$ / 1	Best switch utilization; compact design; high efficiency; wide output range Not modular design; unidirectional operation.
[143] (Fig. 8d)	10 / 0 / 1	Modular design; bidirectional operation. Very poor switch utilization; low efficiency; complex control.
[144] (Fig. 8e)	16 / 4 / 1	Modular design; (potential) bidirectional operation. Poor switch utilization; complex control; high cost; fixed output.

PFC. The following dc/dc stage consists of a half-bridge NPC converter, a high-frequency transformer, and a diode bridge rectifier. The use of the half-bridge NPC converter in the dc/dc stage further reduces the size of the high-frequency transformer. The system efficiency is higher than 97.5% at 50 kW.

Another SST implementation [143], shown in Fig. 8(d), uses a full-bridge ac/dc front end and a DHB converter in the dc/dc stage. To integrate energy storage into the charging station, a nonisolated boost converter is added between the ac/dc front end and the dc/dc stage. Compared with the previous converters, this converter is capable of bidirectional power flow but uses more active switches, which results in poor switch utilization and low efficiency. In addition, the control is more complex than that of the unidirectional converters. The proposed design is only verified on a down-scaled prototype with a 140-V ac input voltage. Similar design using a full-bridge converter as the active front end and current-fed DAB converter as the isolated dc/dc stage can be found in [148]. However, the design from [148] is also verified only at a reduced input voltage. In [149], an SST with a full-bridge converter as an active front end and a DAB converter as the isolated dc/dc stage is constructed with silicon IGBTs. The converter is verified with 3.6-kV input, and the reported efficiency is less than 92%.

Another SST implementation led by Delta Electronics aims at building a three-phase SST-based 400-kW XFC connected to the 4.8- or 13.2-kV MV grid [144]. The proposed topology is shown in Fig. 8(e). Each module is rated at 15 kW with 1-kV ac input voltage. Considering line-to-neutral voltage, three modules are connected in series for 4.8 kV and nine modules for 13.2-kV grid. The ac/dc front end uses a full-bridge NPC converter, while the isolated dc/dc stage is an *LLC* converter. The primary side of the *LLC* converter is a three-level converter, which reduces the stress on the resonant components. The secondary side is an active full-bridge that can operate in synchronous rectification to reduce the losses. The dc output of the *LLC* converter is constant 1 kV, and a subsequent nonisolated dc/dc converter is used to interface the EV battery. All the switches are SiC MOSFETs, which increases the system efficiency but results in higher cost. Bidirectional operation is possible but requires sophisticated

control due to the use of the *LLC* converter. The efficiency of a single module is 97.3% measured at 15-kW and 1-kV ac input.

The modular design with input-series-output-parallel configuration makes the XFC MV ready by using only LV MOSFETs or IGBTs. Redundancy can be achieved by adding more modules. In addition, the multilevel waveform generated by the modular ac/dc front end presents the potential to reduce the size of the passive filters. However, with modular design, the large number of components can increase the size of the system, offsetting the advantage brought by smaller passives. The input series connection implies that balanced voltage sharing between the modules needs to be maintained. The increase in the control complexity and the number of components may lead to lower system reliability.

B. Single-Module Design

The recent advances in high-voltage SiC MOSFETs with blocking voltages of 10–15 kV enable interfacing MV grid directly by using a single-module converter. This significantly reduces the complexity of the system and has the potential of achieving higher system reliability and efficiency.

In [150], a single-module 10-kW SST is designed and implemented to interface a 3.6-kV MV ac input based on 13-kV SiC MOSFETs and junction barrier Schottky (JBS) diodes, as shown in Fig. 9(a). The internal dc bus voltage is 6 kV. To reduce the switching losses of the ac/dc front end, a unipolar modulation with one leg operating as unfolding bridge with line frequency is used. In addition, the switching frequency of the PWM leg is limited to 6 kHz to further reduce the losses. The isolated dc/dc stage is a DHB converter with 13-kV SiC MOSFETs on the primary side. Phase-shift control is used to regulate the output voltage, and zero voltage turn-on is achieved for all MOSFETs. The high-frequency transformer with turns ratio of $N = 15$ converts the MV into an LV at the secondary side. The measured efficiency at 10 kW was 94%.

In [151] and [152], another single-module SST with larger power rating is designed and implemented to interface 3.8-kV MV ac input to 400-V dc bus based on 10-kV SiC MOSFETs, as shown in Fig. 9(b). The ac/dc front end is a full-bridge rectifier with a 7-kV internal bus. Similar to [150], a unipolar

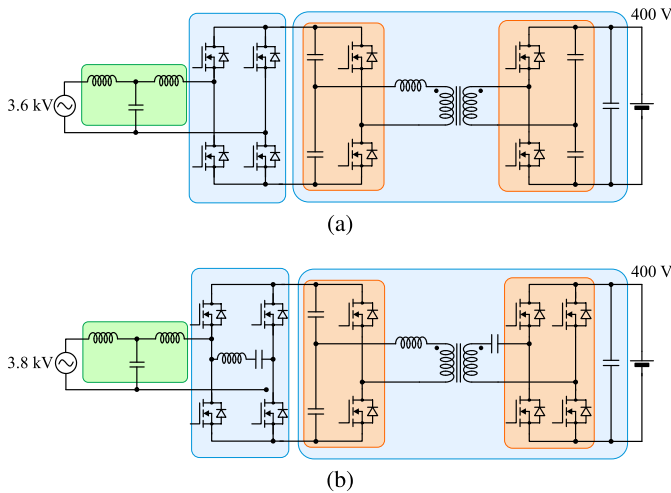


Fig. 9. MV dc fast chargers based on single-module SST technology. (a) MV-interfaced SST proposed in [150]. (b) MV-interfaced SST proposed in [151] and [152].

modulation is adopted for the ac/dc front end to reduce the switching losses. The switching frequency of the PWM leg varies from 35 to 75 kHz. To enable such a high switching frequency at MV, soft-switching over the whole line period is achieved by inserting an LC -branch between the terminals of the two phase legs. The isolated dc/dc stage is an LLC resonant converter with 13-kV SiC MOSFETs half-bridge on the primary side of the high-frequency transformer. The LLC stage operates at a fixed frequency, and the output voltage is regulated by adjusting the internal bus voltage through the ac/dc front end; ZVS is achieved for all MOSFETs. The system efficiency was measured to be 98% at 25 kW.

It is important to point out that power electronics converters interfaced directly with the MV grid as in the case of the SST are subject to relevant protection, safety, and power quality standards for MV equipment [153]–[156] in addition to the current standards for EV chargers such those developed by CHAdeMo, IEC, and SAE [7], [9], [43]–[45]. Connecting power electronics to the MV line introduces a number of issues in terms of safety and protection that need careful mitigation for the successful adoption of this technology.

VI. CONCLUSION

Despite the increasing number of EVs on the road, the lack of charging infrastructure and long charging times restrict the use of these vehicles to daily commutes and short-distance trips. To address this problem, there is a need for a cost-effective and ubiquitous charging infrastructure that can compete with the existing gasoline-powered vehicle-refueling infrastructure.

This article reviews the state-of-the-art XFC converter technology for EVs that can address the challenges and utilize the opportunities brought by the increasing penetration of EVs. An emerging trend is to colocate multiple XFCs to form XFC charging stations and, thus, reduce the installation cost per charging stall. By exploiting the load diversification resulting from different EV battery capacities and different charge

acceptances, a function of the battery SOC, the installation and operation cost can be reduced, bringing benefits to the station owner and the EV users. Energy storage and RES are integrated as part of the charging stations as a common method to reduce high-demand charges that are incurred during peak power hours. It further enables profiling the power exchange between the charging station and the grid, and therefore provides ancillary services to support grid operation.

Two different distribution methods for XFC stations are presented. While the ac distribution method is a mature solution with available components and well-established standards, the dc distribution method presents the potential of achieving lower cost and higher efficiency. The suitable power electronics converters for both methods are reviewed and compared. The major challenge for power electronics converters lies in accommodating the wide output voltage and power range of the EV charging profile while maintaining high efficiency and high power density.

While the state-of-the-art dc fast chargers require MV-to-LV line-frequency transformers, another solution is the SST-based dc fast charger that provides rectification, voltage step-down, and isolation function in a single unit. The SST-based XFCs provide size reduction and efficiency improvement over the state-of-the-art implementations, which can in turn reduce the installation costs by allowing more power delivery on the same station footprint and maximize operating profit by minimizing the power lost in the conversion process.

REFERENCES

- [1] B. Nykvist and M. Nilsson, "Rapidly falling costs of battery packs for electric vehicles," *Nature Climate Change*, vol. 5, no. 4, p. 329, 2015.
- [2] Z. P. Cano *et al.*, "Batteries and fuel cells for emerging electric vehicle markets," *Nature Energy*, vol. 3, no. 4, p. 279, 2018.
- [3] IEA. *Global EV Outlook 2019*. Accessed: Nov. 15, 2019. [Online]. Available: <https://www.iea.org/publications/reports/globaleveoutlook2019/>
- [4] S. Manzetti and F. Mariasiu, "Electric vehicle battery technologies: From present state to future systems," *Renew. Sustain. Energy Rev.*, vol. 51, pp. 1004–1012, Nov. 2015.
- [5] S. Ahmed *et al.*, "Enabling fast charging—A battery technology gap assessment," *J. Power Sources*, vol. 367, pp. 250–262, Nov. 2017.
- [6] M. Keyser *et al.*, "Enabling fast charging—battery thermal considerations," *J. Power Sources*, vol. 367, pp. 228–236, Nov. 2017.
- [7] SAE *Electric Vehicle and Plug in Hybrid Electric Vehicle Conductive Charge Coupler*, Standard SAE J1772, Oct. 2017, p. 1.
- [8] E. Loveday. *Rare Look Inside Tesla Supercharger*. Accessed: Nov. 15, 2019. [Online]. Available: <https://insideevs.com/news/322486/rare-look-inside-tesla-supercharger/>
- [9] *Plugs, Socket-Outlets, Vehicle Connectors and Vehicle Inlets—Conductive Charging of Electric Vehicles—Part 3: Dimensional Compatibility and Interchangeability Requirements for D.C. and A.C./D.C. Pin and Contact-Tube Vehicle Couplers*, Standard IEC 62196-3:2014, Jun. 2014, p. 1.
- [10] A. Yoshida. *Chademo Quick Charger Connector With Excellent Operability*. Accessed: Nov. 15, 2019. [Online]. Available: <https://global-sei.com/technology/tr/bn84/pdf/84-05.pdf>
- [11] A. Burnham *et al.*, "Enabling fast charging—infrastructure and economic considerations," *J. Power Sources*, vol. 367, pp. 237–249, Nov. 2017.
- [12] H. Feng, T. Cai, S. Duan, J. Zhao, X. Zhang, and C. Chen, "An LLC-compensated resonant converter optimized for robust reaction to large coupling variation in dynamic wireless power transfer," *IEEE Trans. Ind. Electron.*, vol. 63, no. 10, pp. 6591–6601, Oct. 2016.
- [13] F. Musavi and W. Eberle, "Overview of wireless power transfer technologies for electric vehicle battery charging," *IET Power Electron.*, vol. 7, no. 1, pp. 60–66, Jan. 2014.

- [14] D. Patil, M. K. McDonough, J. M. Miller, B. Fahimi, and P. T. Balsara, "Wireless power transfer for vehicular applications: Overview and challenges," *IEEE Trans. Transport. Electrification*, vol. 4, no. 1, pp. 3–37, Mar. 2018.
- [15] M. Smith and J. Castellano, "Costs associated with non-residential electric vehicle supply equipment: Factors to consider in the implementation of electric vehicle charging stations," New West Technol., LLC, Portland, OR, USA, Tech. Rep. DOE/EE-1289, 2015.
- [16] Q. Wu, A. H. Nielsen, J. Østergaard, S. T. Cha, and Y. Ding, "Impact study of electric vehicle (EV) integration on medium voltage (MV) grids," in *Proc. 2nd IEEE PES Int. Conf. Exhib. Innov. Smart Grid Technol.*, Dec. 2011, pp. 1–7.
- [17] K. Clement-Nyns, E. Haesen, and J. Driesen, "The impact of charging plug-in hybrid electric vehicles on a residential distribution grid," *IEEE Trans. Power Syst.*, vol. 25, no. 1, pp. 371–380, Feb. 2010.
- [18] M. J. Rutherford and V. Yousefzadeh, "The impact of electric vehicle battery charging on distribution transformers," in *Proc. 26th Annu. IEEE Appl. Power Electron. Conf. Expo. (APEC)*, Mar. 2011, pp. 396–400.
- [19] H. Shareef, M. M. Islam, and A. Mohamed, "A review of the state-of-the-art charging technologies, placement methodologies, and impacts of electric vehicles," *Renew. Sustain. Energy Rev.*, vol. 64, pp. 403–420, 2016.
- [20] C. Capasso and O. Veneri, "Experimental study of a DC charging station for full electric and plug in hybrid vehicles," *Appl. Energy*, vol. 152, pp. 131–142, Aug. 2015.
- [21] D. Sbordone, I. Bertini, B. Di Pietra, M. C. Falvo, A. Genovese, and L. Martirano, "EV fast charging stations and energy storage technologies: A real implementation in the smart micro grid paradigm," *Electr. Power Syst. Res.*, vol. 120, pp. 96–108, Mar. 2015.
- [22] S. Bai, Y. Du, and S. Lukic, "Optimum design of an EV/PHEV charging station with DC bus and storage system," in *Proc. IEEE Energy Convers. Congr. Expo. (ECCE)*, Sep. 2010, pp. 1178–1184.
- [23] J. C. Mukherjee and A. Gupta, "A review of charge scheduling of electric vehicles in smart grid," *IEEE Syst. J.*, vol. 9, no. 4, pp. 1541–1553, Dec. 2015.
- [24] S. Rajakaruna, F. Shahnia, and A. Ghosh, *Plug in Electric Vehicles in Smart Grids: Charging Strategies*. Singapore: Springer, 2014.
- [25] Z. Xu, Z. Hu, Y. Song, Z. Luo, K. Zhan, and J. Wu, "Coordinated charging strategy for PEVs charging stations," in *Proc. IEEE Power Energy Soc. Gen. Meeting*, Jul. 2012, pp. 1–8.
- [26] M. Tabari and A. Yazdani, "An energy management strategy for a DC distribution system for power system integration of plug-in electric vehicles," *IEEE Trans. Smart Grid*, vol. 7, no. 2, pp. 659–668, Mar. 2016.
- [27] S. Negarestani, M. Fotuhi-Firuzabad, M. Rastegar, and A. Rajabi-Ghahnavieh, "Optimal sizing of storage system in a fast charging station for plug-in hybrid electric vehicles," *IEEE Trans. Transport. Electrification*, vol. 2, no. 4, pp. 443–453, Dec. 2016.
- [28] P. You, Z. Yang, M.-Y. Chow, and Y. Sun, "Optimal cooperative charging strategy for a smart charging station of electric vehicles," *IEEE Trans. Power Syst.*, vol. 31, no. 4, pp. 2946–2956, Jul. 2016.
- [29] S. Y. Derakhshandeh, A. S. Masoum, S. Deilami, M. A. S. Masoum, and M. E. Hamedani Golshan, "Coordination of generation scheduling with PEVs charging in industrial microgrids," *IEEE Trans. Power Syst.*, vol. 28, no. 3, pp. 3451–3461, Aug. 2013.
- [30] F. Koyanagi and Y. Uriu, "A strategy of load leveling by charging and discharging time control of electric vehicles," *IEEE Trans. Power Syst.*, vol. 13, no. 3, pp. 1179–1184, Aug. 1998.
- [31] C. D. White and K. M. Zhang, "Using vehicle-to-grid technology for frequency regulation and peak-load reduction," *J. Power Sources*, vol. 196, no. 8, pp. 3972–3980, 2011.
- [32] T. Wu, Q. Yang, Z. Bao, and W. Yan, "Coordinated energy dispatching in microgrid with wind power generation and plug-in electric vehicles," *IEEE Trans. Smart Grid*, vol. 4, no. 3, pp. 1453–1463, Sep. 2013.
- [33] M. Kesler, M. C. Kisacikoglu, and L. M. Tolbert, "Vehicle-to-grid reactive power operation using plug-in electric vehicle bidirectional offboard charger," *IEEE Trans. Ind. Electron.*, vol. 61, no. 12, pp. 6778–6784, Dec. 2014.
- [34] J. Y. Yong, V. K. Ramachandaramurthy, K. M. Tan, and N. Mithulanathan, "Bi-directional electric vehicle fast charging station with novel reactive power compensation for voltage regulation," *Int. J. Elect. Power Energy Syst.*, vol. 64, pp. 300–310, Jan. 2015.
- [35] W. Hu, C. Su, Z. Chen, and B. Bak-Jensen, "Optimal operation of plug-in electric vehicles in power systems with high wind power penetrations," *IEEE Trans. Sustain. Energy*, vol. 4, no. 3, pp. 577–585, Jul. 2013.
- [36] M. Ghofrani, A. Arabali, M. Etezadi-Amoli, and M. S. Fadali, "Smart scheduling and cost-benefit analysis of grid-enabled electric vehicles for wind power integration," *IEEE Trans. Smart Grid*, vol. 5, no. 5, pp. 2306–2313, Sep. 2014.
- [37] Y. Cao, N. Wang, G. Kamel, and Y.-J. Kim, "An electric vehicle charging management scheme based on publish/subscribe communication framework," *IEEE Syst. J.*, vol. 11, no. 3, pp. 1822–1835, Sep. 2017.
- [38] Y. Cao, Y. Miao, G. Min, T. Wang, Z. Zhao, and H. Song, "Vehicular-publish/subscribe (V-P/S) communication enabled on-the-move EV charging management," *IEEE Commun. Mag.*, vol. 54, no. 12, pp. 84–92, Dec. 2016.
- [39] I. S. Bayram, G. Michailidis, M. Devetsikiotis, and F. Granelli, "Electric power allocation in a network of fast charging stations," *IEEE J. Sel. Areas Commun.*, vol. 31, no. 7, pp. 1235–1246, Jul. 2013.
- [40] X. Dong, Y. Mu, H. Jia, J. Wu, and X. Yu, "Planning of fast EV charging stations on a round freeway," *IEEE Trans. Sustain. Energy*, vol. 7, no. 4, pp. 1452–1461, Oct. 2016.
- [41] A. Khaligh and S. Dusmez, "Comprehensive topological analysis of conductive and inductive charging solutions for plug-in electric vehicles," *IEEE Trans. Veh. Technol.*, vol. 61, no. 8, pp. 3475–3489, Oct. 2012.
- [42] M. Yilmaz and P. T. Krein, "Review of battery charger topologies, charging power levels, and infrastructure for plug-in electric and hybrid vehicles," *IEEE Trans. Power Electron.*, vol. 28, no. 5, pp. 2151–2169, May 2013.
- [43] *Electric Vehicle Conductive Charging System—Part 1: General Requirements*, Standard IEC 61851-1:2017, Feb. 2017, pp. 1–287.
- [44] *Electric Vehicle Conductive Charging System—Part 23: DC Electric Vehicle Charging Station*, Standard IEC 61851-23:2014, Mar. 2014, pp. 1–159.
- [45] *Electric Vehicle Conductive Charging System—Part 24: Digital Communication Between A D.C. EV Charging Station and an Electric Vehicle for Control of D.C. Charging*, Standard IEC 61851-24:2014, Mar. 2014, pp. 1–63.
- [46] A. Agius, *What's Involved in the Construction of an Ultra-Rapid Electric Car Charging Station?* [Online]. Available: <https://www.drivezero.com.au/charging/whats-involved-in-the-construction-of-an-ultra-rapid-electric-car-charging-station/>
- [47] S. Bai and S. M. Lukic, "Unified active filter and energy storage system for an MW electric vehicle charging station," *IEEE Trans. Power Electron.*, vol. 28, no. 12, pp. 5793–5803, Dec. 2013.
- [48] M. S. Agamy et al., "An efficient partial power processing DC/DC converter for distributed PV architectures," *IEEE Trans. Power Electron.*, vol. 29, no. 2, pp. 674–686, Feb. 2014.
- [49] W. Yu, J. Lai, H. Ma, and C. Zheng, "High-efficiency DC-DC converter with twin bus for dimmable led lighting," *IEEE Trans. Power Electron.*, vol. 26, no. 8, pp. 2095–2100, Aug. 2011.
- [50] J. Rojas, H. Renaudineau, S. Kouro, and S. Rivera, "Partial power DC-DC converter for electric vehicle fast charging stations," in *Proc. 43rd Annu. Conf. IEEE Ind. Electron. Soc. (IECON)*, Oct. 2017, pp. 5274–5279.
- [51] V. Mahadeva Iyer, S. Gulur, G. Gohil, and S. Bhattacharya, "An approach towards extreme fast charging station power delivery for electric vehicles with partial power processing," *IEEE Trans. Ind. Electron.*, to be published.
- [52] S. Augustine, J. E. Quiroz, M. J. Reno, and S. Brahma, "DC microgrid protection: Review and challenges," Sandia Nat. Lab., Albuquerque, NM, USA, Tech. Rep. SAND2018-8853, 2018.
- [53] D. Salomonsson, L. Söder, and A. Sannino, "Protection of low-voltage DC microgrids," *IEEE Trans. Power Del.*, vol. 24, no. 3, pp. 1045–1053, Jul. 2009.
- [54] D. M. Bui, S. Chen, C. Wu, K. Lien, C. Huang, and K. Jen, "Review on protection coordination strategies and development of an effective protection coordination system for DC microgrid," in *Proc. IEEE PES Asia-Pacific Power Energy Eng. Conf. (APPEEC)*, Dec. 2014, pp. 1–10.
- [55] J.-D. Park and J. Candelaria, "Fault detection and isolation in low-voltage DC-bus microgrid system," *IEEE Trans. Power Del.*, vol. 28, no. 2, pp. 779–787, Apr. 2013.
- [56] D. Meyer and J. Wang, "Integrating ultra-fast charging stations within the power grids of smart cities: A review," *IET Smart Grid*, vol. 1, no. 1, pp. 3–10, 2018.

- [57] B. Singh, B. N. Singh, A. Chandra, K. Al-Haddad, A. Pandey, and D. P. Kothari, "A review of three-phase improved power quality AC-DC converters," *IEEE Trans. Ind. Electron.*, vol. 51, no. 3, pp. 641–660, Jun. 2004.
- [58] J. W. Kolar and T. Friedli, "The essence of three-phase PFC rectifier systems—Part I," *IEEE Trans. Power Electron.*, vol. 28, no. 1, pp. 176–198, Jan. 2013.
- [59] D. Aggeler, F. Canales, H. Zelaya-De La Parra, A. Coccia, N. Butcher, and O. Apeldoorn, "Ultra-fast DC-charge infrastructures for EV-mobility and future smart grids," in *Proc. IEEE PES Innov. Smart Grid Technol. Conf. Eur. (ISGT Eur.)*, Oct. 2010, pp. 1–8.
- [60] T. Kang, C. Kim, Y. Suh, H. Park, B. Kang, and D. Kim, "A design and control of bi-directional non-isolated DC-DC converter for rapid electric vehicle charging system," in *Proc. 27th Annu. IEEE Appl. Power Electron. Conf. Expo. (APEC)*, Feb. 2012, pp. 14–21.
- [61] N. Celanovic and D. Boroyevich, "A comprehensive study of neutral-point voltage balancing problem in three-level neutral-point-clamped voltage source PWM inverters," *IEEE Trans. Power Electron.*, vol. 15, no. 2, pp. 242–249, Mar. 2000.
- [62] S. Rivera, B. Wu, S. Kouro, V. Yaramasu, and J. Wang, "Electric vehicle charging station using a neutral point clamped converter with bipolar DC bus," *IEEE Trans. Ind. Electron.*, vol. 62, no. 4, pp. 1999–2009, Apr. 2015.
- [63] L. Tan, B. Wu, V. Yaramasu, S. Rivera, and X. Guo, "Effective voltage balance control for bipolar-DC-bus-fed EV charging station with three-level DC-DC fast charger," *IEEE Trans. Ind. Electron.*, vol. 63, no. 7, pp. 4031–4041, Jul. 2016.
- [64] J. Kim, J. Lee, T. Eom, K. Bae, M. Shin, and C. Won, "Design and control method of 25 kW high efficient EV fast charger," in *Proc. 21st Int. Conf. Electr. Mach. Syst. (ICEMS)*, Oct. 2018, pp. 2603–2607.
- [65] S. Chen, W. Yu, and D. Meyer, "Design and implementation of forced air-cooled, 140 kHz, 20 kW SiC MOSFET based Vienna PFC," in *Proc. IEEE Appl. Power Electron. Conf. Expo. (APEC)*, Mar. 2019, pp. 1196–1203.
- [66] J. A. Anderson, M. Haider, D. Bortis, J. W. Kolar, M. Kasper, and G. Deboy, "New synergetic control of a 20 kW isolated Vienna rectifier front-end EV battery charger," in *Proc. 20th Workshop Control Modeling Power Electron. (COMPEL)*, Jun. 2019, pp. 1–8.
- [67] T. Nussbaumer, M. Baumann, and J. W. Kolar, "Comprehensive design of a three-phase three-switch buck-type PWM rectifier," *IEEE Trans. Power Electron.*, vol. 22, no. 2, pp. 551–562, Mar. 2007.
- [68] A. Stupar, T. Friedli, J. Miniböck, and J. W. Kolar, "Towards a 99% efficient three-phase buck-type PFC rectifier for 400-V DC distribution systems," *IEEE Trans. Power Electron.*, vol. 27, no. 4, pp. 1732–1744, Apr. 2012.
- [69] B. Guo, F. Wang, and E. Aeloiza, "A novel three-phase current source rectifier with delta-type input connection to reduce the device conduction loss," *IEEE Trans. Power Electron.*, vol. 31, no. 2, pp. 1074–1084, Feb. 2016.
- [70] J. Lei, S. Feng, J. Zhao, W. Chen, P. Wheeler, and M. Shi, "An improved three-phase buck rectifier topology with reduced voltage stress on transistors," *IEEE Trans. Power Electron.*, to be published.
- [71] Y. Du, S. Lukic, B. Jacobson, and A. Huang, "Review of high power isolated bi-directional DC-DC converters for PHEV/EV DC charging infrastructure," in *Proc. IEEE Energy Convers. Congr. Expo. (ECCE)*, Sep. 2011, pp. 553–560.
- [72] P. He and A. Khaligh, "Comprehensive analyses and comparison of 1 kW isolated DC-DC converters for bidirectional EV charging systems," *IEEE Trans. Transport. Electrification*, vol. 3, no. 1, pp. 147–156, Mar. 2017.
- [73] J. A. Sabate, V. Vlatkovic, R. B. Ridley, and F. C. Lee, "High-voltage, high-power, ZVS, full-bridge PWM converter employing an active snubber," in *Proc. 6th Annu. Appl. Power Electron. Conf. Exhib. (APEC)*, Mar. 1991, pp. 158–163.
- [74] J.-G. Cho, J.-W. Baek, C.-Y. Jeong, and G.-H. Rim, "Novel zero-voltage and zero-current-switching full-bridge PWM converter using a simple auxiliary circuit," *IEEE Trans. Ind. Appl.*, vol. 35, no. 1, pp. 15–20, Jan. 1999.
- [75] D. S. Gautam, F. Musavi, W. Eberle, and W. G. Dunford, "A zero-voltage switching full-bridge DC-DC converter with capacitive output filter for plug-in hybrid electric vehicle battery charging," *IEEE Trans. Power Electron.*, vol. 28, no. 12, pp. 5728–5735, Dec. 2013.
- [76] M. Pahlevaninezhad, P. Das, J. Drobniak, P. K. Jain, and A. Bakhshai, "A novel ZVZCS full-bridge DC/DC converter used for electric vehicles," *IEEE Trans. Power Electron.*, vol. 27, no. 6, pp. 2752–2769, Jun. 2012.
- [77] M. Pahlevaninezhad, J. Drobniak, P. K. Jain, and A. Bakhshai, "A load adaptive control approach for a zero-voltage-switching DC/DC converter used for electric vehicles," *IEEE Trans. Ind. Electron.*, vol. 59, no. 2, pp. 920–933, Feb. 2012.
- [78] B. Yang, F. C. Lee, A. J. Zhang, and G. Huang, "LLC resonant converter for front end DC/DC conversion," in *Proc. 17th Annu. IEEE Appl. Power Electron. Conf. Expo. (APEC)*, vol. 2, Mar. 2002, pp. 1108–1112.
- [79] J. E. Huber, J. Miniböck, and J. W. Kolar, "Generic derivation of dynamic model for half-cycle DCM series resonant converters," *IEEE Trans. Power Electron.*, vol. 33, no. 1, pp. 4–7, Jan. 2018.
- [80] I. Lee, "Hybrid DC-DC converter with phase-shift or frequency modulation for NEV battery charger," *IEEE Trans. Ind. Electron.*, vol. 63, no. 2, pp. 884–893, Feb. 2016.
- [81] M. Pahlevani, S. Pan, and P. Jain, "A hybrid phase-shift modulation technique for DC/DC converters with a wide range of operating conditions," *IEEE Trans. Ind. Electron.*, vol. 63, no. 12, pp. 7498–7510, Dec. 2016.
- [82] H. Wang, S. Dusmez, and A. Khaligh, "Maximum efficiency point tracking technique for LLC-based PEV chargers through variable DC link control," *IEEE Trans. Ind. Electron.*, vol. 61, no. 11, pp. 6041–6049, Nov. 2014.
- [83] H. Hu, X. Fang, F. Chen, Z. J. Shen, and I. Batarseh, "A modified high-efficiency LLC converter with two transformers for wide input-voltage range applications," *IEEE Trans. Power Electron.*, vol. 28, no. 4, pp. 1946–1960, Apr. 2013.
- [84] W. Hongfei, L. Yuewei, and X. Yan, "LLC resonant converter with semiaactive variable-structure rectifier (SA-VSR) for wide output voltage range application," *IEEE Trans. Power Electron.*, vol. 31, no. 5, pp. 3389–3394, May 2016.
- [85] Z. Hu, Y. Qiu, L. Wang, and Y.-F. Liu, "An interleaved LLC resonant converter operating at constant switching frequency," *IEEE Trans. Power Electron.*, vol. 29, no. 6, pp. 2931–2943, Jun. 2014.
- [86] A. Coccia, F. Canales, P. Barbosa, and S. Ponnaluri, "Wide input voltage range compensation in DC/DC resonant architectures for on-board traction power supplies," in *Proc. Eur. Conf. Power Electron. Appl.*, Sep. 2007, pp. 1–10.
- [87] Y. Nakahara, H. Otake, T. M. Evans, T. Yoshida, M. Tsuruya, and K. Nakahara, "Three-phase LLC series resonant DC/DC converter using SiC MOSFETs to realize high-voltage and high-frequency operation," *IEEE Trans. Ind. Electron.*, vol. 63, no. 4, pp. 2103–2110, Apr. 2016.
- [88] H.-M. Yoon, J.-H. Kim, and E.-H. Song, "Design of a novel 50 kw fast charger for electric vehicles," *J. Central South Univ.*, vol. 20, no. 2, pp. 372–377, 2013.
- [89] M. N. Kheraluwala, R. W. Gascoigne, D. M. Divan, and E. D. Baumann, "Performance characterization of a high-power dual active bridge DC-to-DC converter," *IEEE Trans. Ind. Appl.*, vol. 28, no. 6, pp. 1294–1301, Nov./Dec. 1992.
- [90] S. Han and D. Divan, "Bi-directional DC/DC converters for plug-in hybrid electric vehicle (PHEV) applications," in *Proc. 23rd Annu. IEEE Appl. Power Electron. Conf. Expo.*, Feb. 2008, pp. 784–789.
- [91] C. Mi, H. Bai, C. Wang, and S. Gargies, "Operation, design and control of dual H-bridge-based isolated bidirectional DC-DC converter," *IET Power Electron.*, vol. 1, no. 4, pp. 507–517, Dec. 2008.
- [92] R. J. Ferreira, L. M. Miranda, R. E. Araújo, and J. P. Lopes, "A new bi-directional charger for vehicle-to-grid integration," in *Proc. 2nd IEEE PES Int. Conf. Exhib. Innov. Smart Grid Technol.*, Dec. 2011, pp. 1–5.
- [93] H. van Hoek, M. Neubert, and R. W. De Doncker, "Enhanced modulation strategy for a three-phase dual active bridge-boosting efficiency of an electric vehicle converter," *IEEE Trans. Power Electron.*, vol. 28, no. 12, pp. 5499–5507, Dec. 2013.
- [94] L. Xue, Z. Shen, D. Boroyevich, P. Mattavelli, and D. Diaz, "Dual active bridge-based battery charger for plug-in hybrid electric vehicle with charging current containing low frequency ripple," *IEEE Trans. Power Electron.*, vol. 30, no. 12, pp. 7299–7307, Dec. 2015.
- [95] L. Xue, M. Mu, D. Boroyevich, and P. Mattavelli, "The optimal design of GaN-based dual active bridge for bi-directional plug-IN hybrid electric vehicle (PHEV) charger," in *Proc. Appl. Power Electron. Conf. Expo. (APEC)*, Mar. 2015, pp. 602–608.
- [96] R. W. De Doncker, D. M. Divan, and M. H. Kheraluwala, "A three-phase soft-switched high power density DC/DC converter for high power applications," in *Proc. Conf. Rec. IEEE Ind. Appl. Soc. Annu. Meeting*, vol. 1, Oct. 1988, pp. 796–805.

- [97] H. Akagi, T. Yamagishi, N. M. L. Tan, S. Kinouchi, Y. Miyazaki, and M. Koyama, "Power-loss breakdown of a 750-V 100-kW 20-kHz bidirectional isolated DC-DC converter using SiC-MOSFET/SBD dual modules," *IEEE Trans. Ind. Appl.*, vol. 51, no. 1, pp. 420–428, Jan. 2015.
- [98] J. E. Huber and J. W. Kolar, "Applicability of solid-state transformers in today's and future distribution grids," *IEEE Trans. Smart Grid*, vol. 10, no. 1, pp. 317–326, Jan. 2019.
- [99] N. M. L. Tan, T. Abe, and H. Akagi, "Design and performance of a bidirectional isolated DC-DC converter for a battery energy storage system," *IEEE Trans. Power Electron.*, vol. 27, no. 3, pp. 1237–1248, Mar. 2012.
- [100] H. Wen, W. Xiao, and B. Su, "Nonactive power loss minimization in a bidirectional isolated DC-DC converter for distributed power systems," *IEEE Trans. Ind. Electron.*, vol. 61, no. 12, pp. 6822–6831, Dec. 2014.
- [101] A. Rodríguez, A. Vázquez, D. G. Lamar, M. M. Hernando, and J. Sebastián, "Different purpose design strategies and techniques to improve the performance of a dual active bridge with phase-shift control," *IEEE Trans. Power Electron.*, vol. 30, no. 2, pp. 790–804, Feb. 2015.
- [102] B. Zhao, Q. Song, W. Liu, and W. Sun, "Current-stress-optimized switching strategy of isolated bidirectional DC-DC converter with dual-phase-shift control," *IEEE Trans. Ind. Electron.*, vol. 60, no. 10, pp. 4458–4467, Oct. 2013.
- [103] G. Oggier, G. O. García, and A. R. Oliva, "Modulation strategy to operate the dual active bridge DC-DC converter under soft switching in the whole operating range," *IEEE Trans. Power Electron.*, vol. 26, no. 4, pp. 1228–1236, Apr. 2011.
- [104] F. Krismer and J. W. Kolar, "Efficiency-optimized high-current dual active bridge converter for automotive applications," *IEEE Trans. Ind. Electron.*, vol. 59, no. 7, pp. 2745–2760, Jul. 2012.
- [105] J. Huang, Y. Wang, Z. Li, and W. Lei, "Unified triple-phase-shift control to minimize current stress and achieve full soft-switching of isolated bidirectional DC-DC converter," *IEEE Trans. Ind. Electron.*, vol. 63, no. 7, pp. 4169–4179, Jul. 2016.
- [106] J. Hiltunen, V. Väisänen, R. Juntunen, and P. Silventoinen, "Variable-frequency phase shift modulation of a dual active bridge converter," *IEEE Trans. Power Electron.*, vol. 30, no. 12, pp. 7138–7148, Dec. 2015.
- [107] G. G. Oggier and M. Ordóñez, "High-efficiency DAB converter using switching sequences and burst mode," *IEEE Trans. Power Electron.*, vol. 31, no. 3, pp. 2069–2082, Mar. 2016.
- [108] A. Taylor, G. Liu, H. Bai, A. Brown, P. M. Johnson, and M. McAmmond, "Multiple-phase-shift control for a dual active bridge to secure zero-voltage switching and enhance light-load performance," *IEEE Trans. Power Electron.*, vol. 33, no. 6, pp. 4584–4588, Jun. 2018.
- [109] W. Chen, P. Rong, and Z. Lu, "Snubberless bidirectional DC-DC converter with new CLLC resonant tank featuring minimized switching loss," *IEEE Trans. Ind. Electron.*, vol. 57, no. 9, pp. 3075–3086, Sep. 2010.
- [110] Z. U. Zahid, Z. M. Dalala, R. Chen, B. Chen, and J.-S. Lai, "Design of bidirectional DC-DC resonant converter for vehicle-to-grid (V2G) applications," *IEEE Trans. Transport. Electrification*, vol. 1, no. 3, pp. 232–244, Oct. 2015.
- [111] J.-H. Jung, H.-S. Kim, M.-H. Ryu, and J.-W. Baek, "Design methodology of bidirectional CLLC resonant converter for high-frequency isolation of DC distribution systems," *IEEE Trans. Power Electron.*, vol. 28, no. 4, pp. 1741–1755, Apr. 2013.
- [112] S. Zhao, Q. Li, F. C. Lee, and B. Li, "High-frequency transformer design for modular power conversion from medium-voltage AC to 400 VDC," *IEEE Trans. Power Electron.*, vol. 33, no. 9, pp. 7545–7557, Sep. 2018.
- [113] C.-S. Wang, S.-H. Zhang, Y.-F. Wang, B. Chen, and J.-H. Liu, "A 5-kW isolated high voltage conversion ratio bidirectional CLTC resonant DC-DC converter with wide gain range and high efficiency," *IEEE Trans. Power Electron.*, vol. 34, no. 1, pp. 340–355, Jan. 2019.
- [114] J. Huang et al., "Robust circuit parameters design for the CLLC-type DC transformer in the hybrid AC-DC microgrid," *IEEE Trans. Ind. Electron.*, vol. 66, no. 3, pp. 1906–1918, Mar. 2019.
- [115] B. Li, Q. Li, F. C. Lee, Z. Liu, and Y. Yang, "A high-efficiency high-density wide-bandgap device-based bidirectional on-board charger," *IEEE J. Emerg. Sel. Topics Power Electron.*, vol. 6, no. 3, pp. 1627–1636, Sep. 2018.
- [116] P. He and A. Khaligh, "Design of 1 kW bidirectional half-bridge CLLC converter for electric vehicle charging systems," in *Proc. IEEE Int. Conf. Power Electron., Drives Energy Syst. (PEDES)*, Dec. 2016, pp. 1–6.
- [117] C. Zhang, P. Li, Z. Kan, X. Chai, and X. Guo, "Integrated half-bridge CLLC bidirectional converter for energy storage systems," *IEEE Trans. Ind. Electron.*, vol. 65, no. 5, pp. 3879–3889, May 2018.
- [118] F. Z. Peng, H. Li, G.-J. Su, and J. S. Lawler, "A new ZVS bidirectional DC-DC converter for fuel cell and battery application," *IEEE Trans. Power Electron.*, vol. 19, no. 1, pp. 54–65, Jan. 2004.
- [119] H. Li, D. Liu, F. Z. Peng, and G.-J. Su, "Small signal analysis of a dual half bridge isolated ZVS bi-directional DC-DC converter for electrical vehicle applications," in *Proc. IEEE 36th Power Electron. Spec. Conf.*, Jun. 2005, pp. 2777–2782.
- [120] D. Liu and H. Li, "Design and implementation of a DSP based digital controller for a dual half bridge isolated bi-directional DC-DC converter," in *Proc. 21st Annu. IEEE Appl. Power Electron. Conf. Expo. (APEC)*, Mar. 2006, p. 5.
- [121] O. García, P. Zumel, A. de Castro, and J. A. Cobos, "Automotive DC-DC bidirectional converter made with many interleaved buck stages," *IEEE Trans. Power Electron.*, vol. 21, no. 3, pp. 578–586, May 2006.
- [122] J. Zhang, J.-S. Lai, R.-Y. Kim, and W. Yu, "High-power density design of a soft-switching high-power bidirectional DC-DC converter," *IEEE Trans. Power Electron.*, vol. 22, no. 4, pp. 1145–1153, Jul. 2007.
- [123] D. Christen, F. Jauch, and J. Biel, "Ultra-fast charging station for electric vehicles with integrated split grid storage," in *Proc. 17th Eur. Conf. Power Electron. Appl. (EPE ECCE-Eur.)*, Sep. 2015, pp. 1–11.
- [124] M. T. Zhang, Y. Jiang, F. C. Lee, and M. M. Jovanovic, "Single-phase three-level boost power factor correction converter," in *Proc. 10th Annu. IEEE Appl. Power Electron. Conf. Expo.*, vol. 1, Mar. 1995, pp. 434–439.
- [125] P. J. Grbovic, P. Delarue, P. Le Moigne, and P. Bartholomeus, "A bidirectional three-level DC-DC converter for the ultracapacitor applications," *IEEE Trans. Ind. Electron.*, vol. 57, no. 10, pp. 3415–3430, Oct. 2010.
- [126] S. Dusmez, A. Hasanzadeh, and A. Khaligh, "Comparative analysis of bidirectional three-level DC-DC converter for automotive applications," *IEEE Trans. Ind. Electron.*, vol. 62, no. 5, pp. 3305–3315, May 2015.
- [127] R. M. Cuzner, A. R. Bendre, P. J. Faill, and B. Semenov, "Implementation of a non-isolated three level DC/DC converter suitable for high power systems," in *Proc. IEEE Ind. Appl. Annu. Meeting*, Sep. 2007, pp. 2001–2008.
- [128] L. Tan, N. Zhu, and B. Wu, "An integrated inductor for eliminating circulating current of parallel three-level DC-DC converter-based EV fast charger," *IEEE Trans. Ind. Electron.*, vol. 63, no. 3, pp. 1362–1371, Mar. 2016.
- [129] Y. Du, X. Zhou, S. Bai, S. Lukic, and A. Huang, "Review of non-isolated bi-directional DC-DC converters for plug-in hybrid electric vehicle charge station application at municipal parking decks," in *Proc. 25th Annu. IEEE Appl. Power Electron. Conf. Expo. (APEC)*, Feb. 2010, pp. 1145–1151.
- [130] L. Tan, B. Wu, S. Rivera, and V. Yaramasu, "Comprehensive DC power balance management in high-power three-level DC-DC converter for electric vehicle fast charging," *IEEE Trans. Power Electron.*, vol. 31, no. 1, pp. 89–100, Jan. 2016.
- [131] Z. Zhang et al., "High-efficiency silicon carbide (SiC) converter using paralleled discrete devices in energy storage systems," in *Proc. IEEE Energy Convers. Congr. Expo. (ECCE)*, Sep. 2019, pp. 2471–2477.
- [132] W. Qian, H. Cha, F. Z. Peng, and L. M. Tolbert, "55-kW variable 3X DC-DC converter for plug-in hybrid electric vehicles," *IEEE Trans. Power Electron.*, vol. 27, no. 4, pp. 1668–1678, Apr. 2012.
- [133] J. W. Kolar and J. E. Huber, "Solid-state transformers—Key design challenges, applicability, and future concepts," in *Proc. 17th Int. Conf. Power Electron. Motion Control (PEMC)*, Varna, Bulgaria, Sep. 2016, p. 26.
- [134] Q. Zhu, L. Wang, A. Q. Huang, K. Booth, and L. Zhang, "7.2-kV single-stage solid-state transformer based on the current-fed series resonant converter and 15-kV SiC MOSFETs," *IEEE Trans. Power Electron.*, vol. 34, no. 2, pp. 1099–1112, Feb. 2019.
- [135] X. She, A. Q. Huang, S. Lukic, and M. E. Baran, "On integration of solid-state transformer with zonal DC microgrid," *IEEE Trans. Smart Grid*, vol. 3, no. 2, pp. 975–985, Jun. 2012.

- [136] X. Yu, X. She, X. Zhou, and A. Q. Huang, "Power management for DC microgrid enabled by solid-state transformer," *IEEE Trans. Smart Grid*, vol. 5, no. 2, pp. 954–965, Mar. 2014.
- [137] X. She, A. Q. Huang, and R. Burgos, "Review of solid-state transformer technologies and their application in power distribution systems," *IEEE J. Emerg. Sel. Topics Power Electron.*, vol. 1, no. 3, pp. 186–198, Sep. 2013.
- [138] A. Q. Huang, "Medium-voltage solid-state transformer: Technology for a smarter and resilient grid," *IEEE Ind. Electron. Mag.*, vol. 10, no. 3, pp. 29–42, Sep. 2016.
- [139] *Utility Direct Medium Voltage DC Fast Charger Update: DC Fast Charger Characterization*, EPRI, Palo Alto, CA, USA, Dec. 2012.
- [140] A. Maitra, S. Rajagopalan, J.-S. Lai, M. DuVall, and M. McGranaghan, "Medium voltage stand alone DC fast charger," U.S. Patent Appl. 13/479 389, May 30, 2013.
- [141] J.-S. Lai, W.-H. Lai, S.-R. Moon, L. Zhang, and A. Maitra, "A 15-kV class intelligent universal transformer for utility applications," in *Proc. IEEE Appl. Power Electron. Conf. Expo. (APEC)*, Mar. 2016, pp. 1974–1981.
- [142] S. Srdic, C. Zhang, X. Liang, W. Yu, and S. Lukic, "A SiC-based power converter module for medium-voltage fast charger for plug-in electric vehicles," in *Proc. IEEE Appl. Power Electron. Conf. Expo. (APEC)*, Mar. 2016, pp. 2714–2719.
- [143] M. Vasiladiotis and A. Rufer, "A modular multiport power electronic transformer with integrated split battery energy storage for versatile ultrafast EV charging stations," *IEEE Trans. Ind. Electron.*, vol. 62, no. 5, pp. 3213–3222, May 2015.
- [144] C. Zhu, *High-Efficiency, Medium-Voltage-Input, Solid-State-Transformer-Based 400-kW/1000-V/400-A Extreme Fast Charger for Electric Vehicles*. [Online]. Available: https://www.energy.gov/sites/prod/files/2019/06/f64/elt241_zhu_2019_o_4.24_9.31pm_jl.pdf
- [145] S. Srdic, X. Liang, C. Zhang, W. Yu, and S. Lukic, "A SiC-based high-performance medium-voltage fast charger for plug-in electric vehicles," in *Proc. IEEE Energy Convers. Congr. Expo. (ECCE)*, Sep. 2016, pp. 1–6.
- [146] X. Liang, C. Zhang, S. Srdic, and S. M. Lukic, "Predictive control of a series-interleaved multicell three-level boost power-factor-correction converter," *IEEE Trans. Power Electron.*, vol. 33, no. 10, pp. 8948–8960, Oct. 2018.
- [147] D. Rothmund, G. Ortiz, and J. W. Kolar, "SiC-based unidirectional solid-state transformer concepts for directly interfacing 400 V DC to medium-voltage AC distribution systems," in *Proc. IEEE 36th Int. Telecommun. Energy Conf. (INTELEC)*, Sep./Oct. 2014, pp. 1–9.
- [148] D. Sha, G. Xu, and Y. Xu, "Utility direct interfaced charger/discharger employing unified voltage balance control for cascaded H-bridge units and decentralized control for CF-DAB modules," *IEEE Trans. Ind. Electron.*, vol. 64, no. 10, pp. 7831–7841, Oct. 2017.
- [149] X. She, X. Yu, F. Wang, and A. Q. Huang, "Design and demonstration of a 3.6-kV-120-V/10-kVA solid-state transformer for smart grid application," *IEEE Trans. Power Electron.*, vol. 29, no. 8, pp. 3982–3996, Aug. 2014.
- [150] F. Wang, G. Wang, A. Huang, W. Yu, and X. Ni, "Design and operation of a 3.6 kV high performance solid state transformer based on 13 kV SiC MOSFET and JBS diode," in *Proc. IEEE Energy Convers. Congr. Expo. (ECCE)*, Sep. 2014, pp. 4553–4560.
- [151] D. Rothmund, T. Guillod, D. Bortis, and J. W. Kolar, "99.1% efficient 10 kV SiC-based medium-voltage ZVS bidirectional single-phase PFC AC/DC stage," *IEEE J. Emerg. Sel. Topics Power Electron.*, vol. 7, no. 2, pp. 779–797, Jun. 2019.
- [152] D. Rothmund, T. Guillod, D. Bortis, and J. W. Kolar, "99% efficient 10 kV SiC-based 7 kV/400 V DC transformer for future data centers," *IEEE J. Emerg. Sel. Topics Power Electron.*, vol. 7, no. 2, pp. 753–767, Jun. 2019.
- [153] *IEEE Recommended Practice and Requirements for Harmonic Control in Electric Power Systems*, IEEE Standard 519-2014, Jun. 2014, pp. 1–29.
- [154] *IEEE Standard for General Requirements for Dry-Type Distribution and Power Transformers*, IEEE Standard C57.12.01-2015, Feb. 2015, pp. 1–52.
- [155] *Electromagnetic Compatibility (EMC)—Part 2-12: Environment—Compatibility Levels for Low-Frequency Conducted Disturbances and Signalling in Public Medium-Voltage Power Supply Systems*, Standard IEC 61000-2-12:2003, Apr. 2003, pp. 1–55.
- [156] *Electromagnetic Compatibility (EMC)—Part 3-6: Limits—Assessment of Emission Limits for the Connection of Distorting Installations to MV, HV and EHV Power Systems*, Standard IEC TR 61000-3-6:2008, Feb. 2008, pp. 1–58.



Hao Tu (S'17) received the bachelor's degree from Xi'an Jiaotong University, Xi'an, China, in 2012, and the master's degree from RWTH Aachen University, Aachen, Germany, in 2015, both in electrical engineering. He is currently pursuing the Ph.D. degree in electrical engineering with the Future Renewable Electric Energy Delivery and Management (FREEDM) Systems Center, North Carolina State University, Raleigh, NC, USA.

His research interests include control of power electronics converters, energy storage systems, and microgrids.



Hao Feng (M'19) received the B.S. and Ph.D. degrees from the Huazhong University of Science and Technology, Wuhan, China, in 2013 and 2018, respectively.

Since 2018, he has been with the Future Renewable Electric Energy Delivery and Management (FREEDM) Systems Center, Department of Electrical and Computer Engineering, North Carolina State University, Raleigh, NC, USA, as a Post-Doctoral Researcher. His research interests include inductive power transfer systems, bidirectional dc-dc converters, and medium-voltage power conversion.



Srdjan Srdic (M'09–SM'17) received the B.S., M.S., and Ph.D. degrees in electrical engineering from the University of Belgrade, Belgrade, Serbia, in 2004, 2010, and 2013, respectively.

From 2005 to 2015, he was with the Department of Power Engineering, School of Electrical Engineering, University of Belgrade, where he served as a Teaching Assistant and an Assistant Professor. From 2015 to 2018, he was with North Carolina State University, Raleigh, NC, USA, as a Research Assistant Professor. He is currently with EGSTON Power Electronics GmbH, Vienna, Austria, where he serves as the Director of the Research and Development. His research interests include power hardware-in-the-loop systems and SiC-based medium- and low-voltage power converters for automotive industry and renewable energy applications.



Srdjan Lukic (SM'19) received the Ph.D. degree in electrical engineering from the Illinois Institute of Technology, Chicago, IL, USA, in 2008.

He is currently a Professor with the Department of Electrical and Computer Engineering, North Carolina State University, Raleigh, NC, USA, where he serves as the Deputy Director of the National Science Foundation Future Renewable Electric Energy Delivery and Management (FREEDM) Systems Engineering Research Center.

His research interests include design and control of power electronic converters and electromagnetic energy conversion with application to microgrids, wireless power transfer, energy storage systems, and electric automotive systems.

Dr. Lukic was a Distinguished Lecturer with the IEEE Vehicular Technology Society from 2011 to 2015.